immunostimulant patch. Vaccine 2005;23:946-50

26. Yagi H, Hashizume H, Horibe T, et al. Induction of therapeutically relevant cytotoxic T lymphocytes in humans by percutaneous peptide immunization. Cancer Res 2006;66:10136-44

27. Vogt A, Mahe B, Costagliola D, et al. Transcutaneous anti-influenza vaccination promotes both CD4 and CD8 T cell immune responses in humans. J Immunol 2008;180:1482-9

28. Combadiere B, Vogt A, Mahe B, et al. Preferential amplification of CD8 effector-T cells after transcutaneous application of an inactivated influenza vaccine: a randomized phase I trial. PLoS One 2010;5:e10818

29. Ishii Y, Nakae T, Sakamoto F, et al. A transcutaneous vaccination system using a hydrogel patch for viral and bacterial infection. J Control Release 2008;131:113-20

30. Matsuo K, Ishii Y, Quan YS, et al. Transcutaneous vaccination using a hydrogel patch induces effective immune responses to tetanus and diphtheria toxoid in hairless rat. J Control Release 2011;149:15-20

31. Matsuo K, Ishii Y, Quan YS, et al. Compositional optimization and safety assessment of a hydrogel patch as a transcutaneous immunization device. Biol Pharm Bull 2011;34:1835-40

32. Matsuo K, Ishii Y, Quan YS, et al. Characterization of transcutaneous protein delivery by a hydrogel patch in animal, human, and tissue-engineered skin models. Biol Pharm Bull 2011;34:586-9

33. Hirobe S, Matsuo K, Quan YS, et al. Clinical study of transcutaneous vaccination using a hydrogel patch for tetanus and diphtheria. Vaccine 2012;30:1847-54

34. Kohli AK, Alpar HO. Potential use of nanoparticles for transcutaneous vaccine delivery: effect of particle size and charge. Int J Pharm 2004;275:13-17

35. Shaker DS, Sloat BR, Le UM, et al. Immunization by application of DNA vaccine onto a skin area wherein the hair follicles have been induced into anagen-onset stage. Mol Ther 2007;15:2037-43

36. Vogt A, Combadiere B, Hadam S, et al. 40 nm, but not 750 or 1,500 nm, nanoparticles enter epidermal CD1a+ cells after transcutaneous application on human skin. J Invest Dermatol 2006;126:1316-22

37. Schlosser E, Mueller M, Fischer S, et al. TLR ligands and antigen need to be coencapsulated into the same biodegradable microsphere for the generation of potent cytotoxic T lymphocyte responses. Vaccine 2008;26:1626-37

38. Panyam J, Labhasetwar V. Biodegradable nanoparticles for drug and gene delivery to cells and tissue. Adv Drug Deliv Rev 2003;55:329-47

39. Mattheolabakis G, Lagoumintzis G, Panagi Z, et al. Transcutaneous delivery of a nanoencapsulated antigen: induction of immune responses. Int J Pharm 2010;385:187-93

40. Nagpal K, Singh SK, Mishra DN. Chitosan nanoparticles: a promising system in novel drug delivery. Chem Pharm Bull (Tokyo) 2010;58:1423-30

41. Prego C, Paolicelli P, Diaz B, et al. Chitosan-based nanoparticles for improving immunization against hepatitis B infection. Vaccine 2010;28:2607-14

42. Bal SM, Slutter B, Jiskoot W, et al. Small is beautiful: N-trimethyl chitosan-ovalbumin conjugates for microneedle-based transcutaneous immunisation. Vaccine 2011;29:4025-32

43. Bal SM, Slutter B, van Riet E, et al. Efficient induction of immune responses through intradermal vaccination with N-trimethyl chitosan containing antigen formulations. J Control Release 2010;142:374-83

44. Bal SM, Ding Z, Kersten GF, et al. Microneedle-based transcutaneous immunisation in mice with N-trimethyl chitosan adjuvanted diphtheria toxoid formulations. Pharm Res 2010;27:1837-47

45. El Maghraby GM, Williams AC, Barry BW. Interactions of surfactants (edge activators) and skin penetration enhancers with liposomes. Int J Pharm 2004;276:143-61

46. Paul A, Cevc G, Bachhawat BK. Transdermal immunization with large proteins by means of ultradeformable drug carriers. Eur J Immunol 1995;25:3521-4

47. Paul A, Cevc G, Bachhawat BK. Transdermal immunisation with an integral membrane component, gap junction protein, by means of ultradeformable drug carriers, transfersomes. Vaccine 1998;16:188-95

48. Gupta PN, Mishra V, Rawat A, et al. Non-invasive vaccine delivery in transfersomes, niosomes and liposomes: a comparative study. Int J Pharm 2005;293:73-82

49. Mishra D, Mishra PK, Dubey V, et al. Systemic and mucosal immune response induced by transcutaneous immunization using Hepatitis B surface antigen-loaded modified liposomes. Eur J Pharm Sci 2008;33:424-33

50. Jain S, Vyas SP. Mannosylated niosomes as carrier adjuvant system for topical immunization. J Pharm Pharmacol 2005;57:1177-84

51. Dahlan A, Alpar HO, Stickings P, et al. Transcutaneous immunisation assisted by low-frequency ultrasound. Int J Pharm 2009;368:123-8

52. Tezel A, Paliwal S, Shen Z, et al. Low-frequency ultrasound as a transcutaneous immunization adjuvant. Vaccine 2005;23:3800-7

53. Dahlan A, Alpar HO, Murdan S. An investigation into the combination of low frequency ultrasound and liposomes on skin permeability. Int J Pharm 2009;379:139-42

54. Weaver JC. Electroporation theory. Concepts and mechanisms. Methods Mol Biol 1995;55:3-28

55. Prausnitz MR, Bose VG, Langer R, et al. Electroporation of mammalian skin: a mechanism to enhance transdermal drug delivery. Proc Natl Acad Sci USA 1993;90:10504-8

56. Vanbever R, Lecouturier N, Preat V. Transdermal delivery of metoprolol by electroporation. Pharm Res 1994;11:1657-62

57. Zhao YL, Murthy SN, Manjili MH, et al. Induction of cytotoxic T-lymphocytes by electroporation-enhanced needle-free skin immunization. Vaccine 2006;24:1282-90

58. Cristillo AD, Weiss D, Hudacik L, et al. Persistent antibody and T cell responses induced by HIV-1 DNA vaccine delivered by electroporation. Biochem Biophys Res Commun 2008;366:29-35

RIGHTSLINK

59. Hirao LA, Wu L, Khan AS, et al. Intradermal/subcutaneous immunization by electroporation improves plasmid vaccine delivery and potency in pigs and rhesus macaques. Vaccine 2008;26:440-8
60. Macklin MD, McCabe D, McGregor MW, et al. Immunization of pigs with a particle-mediated DNA vaccine to influenza A virus protects against challenge with homologous virus. J Virol 1998;72:1491-6
61. Chen D, Zuleger C, Chu Q, et al. Epidermal powder immunization with a recombinant HIV gp120 targets Langerhans cells and induces enhanced immune responses. AIDS Res Hum Retroviruses 2002;18:715-22
62. Kelly K, Loskutov A, Zehrung D, et al. Preventing contamination between injections with multiple-use nozzle needle-free injectors: a safety trial. Vaccine 2008;26:1344-52
63. Chen D, Weis KF, Chu Q, et al. Epidermal powder immunization induces both cytotoxic T-lymphocyte and antibody responses to protein antigens of influenza and hepatitis B viruses. J Virol 2001;75:11630-40
64. Chen D, Endres R, Maa YF, et al. Epidermal powder immunization of mice and monkeys with an influenza vaccine. Vaccine 2003;21:2830-6
65. Roberts LK, Barr LJ, Fuller DH, et al. Clinical safety and efficacy of a powdered Hepatitis B nucleic acid vaccine delivered to the epidermis by a commercial prototype device. Vaccine 2005;23:4867-78
66. Drape RJ, Macklin MD, Barr LJ, et al. Epidermal DNA vaccine for influenza is immunogenic in humans. Vaccine 2006;24:4475-81
67. Dincer Z, Jones S, Haworth R. Preclinical safety assessment of a DNA vaccine using particle-mediated epidermal delivery in domestic pig, minipig and mouse. Exp Toxicol Pathol 2006;57:351-7
68. Cassaday RD, Sondel PM, King DM, et al. A phase I study of immunization using particle-mediated epidermal delivery of genes for gp100 and GM-CSF into uninvolved skin of melanoma patients. Clin Cancer Res 2007;13:540-9
69. Braun RP, Dong L, Jerome S, et al. Multi-antigenic DNA immunization using herpes simplex virus type 2 genomic fragments. Hum Vaccin 2008;4:36-43
70. Jones S, Evans K, McElwaine-Johnn H, et al. DNA vaccination protects against an influenza challenge in a double-blind randomised placebo-controlled phase 1b clinical trial. Vaccine 2009;27:2506-12
71. Wang R, Epstein J, Baraceros FM, et al. Induction of CD4(+) T cell-dependent CD8(+) type 1 responses in humans by a malaria DNA vaccine. Proc Natl Acad Sci USA 2001;98:10817-22
72. Epstein JE, Gorak EJ, Charoenvit Y, et al. Safety, tolerability, and lack of antibody responses after administration of a PfCSP DNA malaria vaccine via needle or needle-free jet injection, and comparison of intramuscular and combination intramuscular/intradermal routes. Hum Gene Ther 2002;13:1551-60
73. Williams J, Fox-Leyva L, Christensen C, et al. Hepatitis A vaccine administration: comparison between jet-injector and needle injection. Vaccine 2000;18:1939-43
74. Aboud S, Nilsson C, Karlen K, et al. Strong HIV-specific CD4+ and CD8+ T-lymphocyte proliferative responses in healthy individuals immunized with an HIV-1 DNA vaccine and boosted with recombinant modified vaccinia virus ankara expressing HIV-1 genes. Clin Vaccine Immunol 2010;17:1124-31
75. Belshe RB, Newman FK, Cannon J, et al. Serum antibody responses after intradermal vaccination against influenza. N Engl J Med 2004;351:2286-94

•• **Benefit of transcutaneous vaccination.**

76. Kenney RT, Frech SA, Muenz LR, et al. Dose sparing with intradermal injection of influenza vaccine. N Engl J Med 2004;351:2295-301

•• **Benefit of transcutaneous vaccination.**

77. BD SoulviaTM Prefillable Microinjection System. Available from: http://www.bd.com/pharmaceuticals/products/microinjection.asp
78. Laurent PE, Bonnet S, Alchas P, et al. Evaluation of the clinical performance of a new intradermal vaccine administration technique and associated delivery system. Vaccine 2007;25:8833-42
79. Prymula R, Usluer G, Altinel S, et al. Acceptance and opinions of Intanza/IDflu intradermal influenza vaccine in the Czech Republic and Turkey. Adv Ther 2012;29:41-52
80. Gerstel MS, Place VA. Drug delivery device. US Patent No. 3 1976;964:482
81. Reihsner R, Balogh B, Menzel EJ. Two-dimensional elastic properties of human skin in terms of an incremental model at the in vivo configuration. Med Eng Phys 1995;17:304-13
82. Widera G, Johnson J, Kim L, et al. Effect of delivery parameters on immunization to ovalbumin following intracutaneous administration by a coated microneedle array patch system. Vaccine 2006;24:1653-64
83. Martanto W, Moore JS, Kashlan O, et al. Microinfusion using hollow microneedles. Pharm Res 2006;23:104-13
84. Martanto W, Moore JS, Couse T, et al. Mechanism of fluid infusion during microneedle insertion and retraction. J Control Release 2006;112:357-61
85. Davis SP, Landis BJ, Adams ZH, et al. Insertion of microneedles into skin: measurement and prediction of insertion force and needle fracture force. J Biomech 2004;37:1155-63
86. Donnelly RF, Raj Singh TR, Woolfson AD. Microneedle-based drug delivery systems: microfabrication, drug delivery, and safety. Drug Deliv 2010;17:187-207
87. Prausnitz MR, Langer R. Transdermal drug delivery. Nat Biotechnol 2008;26:1261-8
88. Prausnitz MR, Mikszta JA, Cormier M, et al. Microneedle-based vaccines. Curr Top Microbiol Immunol 2009;333:369-93
89. Henry S, McAllister DV, Allen MG, et al. Microfabricated microneedles: a novel approach to transdermal drug delivery. J Pharm Sci 1998;87:922-5

•• **First proof of concept about microneedle study.**

90. Banks SL, Pinninti RR, Gill HS, et al. Flux across [corrected] microneedle-treated skin is increased by increasing charge of naltrexone and naltrexol in vitro. Pharm Res 2008;25:1677-85
91. Verbaan FJ, Bal SM, van den Berg DJ, et al. Improved piercing of microneedle

RIGHTSLINK

arrays in dermatomed human skin by an impact insertion method. J Control Release 2008;128:80-8

92. Ding Z, Verbaan FJ, Bivas-Benita M, et al. Microneedle arrays for the transcutaneous immunization of diphtheria and influenza in BALB/c mice. J Control Release 2009;136:71-8

93. Ding Z, Van Riet E, Romeijn S, et al. Immune modulation by adjuvants combined with diphtheria toxoid administered topically in BALB/c mice after microneedle array pretreatment. Pharm Res 2009;26:1635-43

94. Mikszta JA, Alarcon JB, Brittingham JM, et al. Improved genetic immunization via micromechanical disruption of skin-barrier function and targeted epidermal delivery. Nat Med 2002;8:415-19

95. McAllister DV, Wang PM, Davis SP, et al. Microfabricated needles for transdermal delivery of macromolecules and nanoparticles: fabrication methods and transport studies. Proc Natl Acad Sci USA 2003;100:13755-60

96. Van Damme P, Oosterhuis-Kafeja F, Van der Wielen M, et al. Safety and efficacy of a novel microneedle device for dose sparing intradermal influenza vaccination in healthy adults. Vaccine 2009;27:454-9

- **Clinical study against infection disease using microneedle device.**

97. Matriano JA, Cormier M, Johnson J, et al. Macroflux microprojection array patch technology: a new and efficient approach for intracutaneous immunization. Pharm Res 2002;19:63-70

98. Gill HS, Prausnitz MR. Coated microneedles for transdermal delivery. J Control Release 2007;117:227-37

99. Zhu Q, Zarnitsyn VG, Ye L, et al. Immunization by vaccine-coated microneedle arrays protects against lethal influenza virus challenge. Proc Natl Acad Sci USA 2009;106:7968-73

100. Chen X, Prow TW, Crichton ML, et al. Dry-coated microprojection array patches for targeted delivery of immunotherapeutics to the skin. J Control Release 2009;139:212-20

101. Gill HS, Prausnitz MR. Coating formulations for microneedles. Pharm Res 2007;24:1369-80

102. Kim YC, Quan FS, Compans RW, et al. Formulation and coating of microneedles with inactivated influenza virus to improve vaccine stability and immunogenicity. J Control Release 2010;142:187-95

103. Kim YC, Quan FS, Compans RW, et al. Stability kinetics of influenza vaccine coated onto microneedles during drying and storage. Pharm Res 2011;28:135-44

104. Hooper JW, Golden JW, Ferro AM, et al. Smallpox DNA vaccine delivered by novel skin electroporation device protects mice against intranasal poxvirus challenge. Vaccine 2007;25:1814-23

105. Miyano T, Tobinaga Y, Kanno T, et al. Sugar micro needles as transdermic drug delivery system. Biomed Microdevices 2005;7:185-8

106. Ito Y, Hagiwara E, Saeki A, et al. Feasibility of microneedles for percutaneous absorption of insulin. Eur J Pharm Sci 2006;29:82-8

107. Ito Y, Yoshimitsu J, Shiroyama K, et al. Self-dissolving microneedles for the percutaneous absorption of EPO in mice. J Drug Target 2006;14:255-61

108. Sullivan SP, Koutsonanos DG, Del Pilar Martin M, et al. Dissolving polymer microneedle patches for influenza vaccination. Nat Med 2010;16:915-20

109. Matsuo K, Yokota Y, Zhai Y, et al. A low-invasive and effective transcutaneous immunization system using a novel dissolving microneedle array for soluble and particulate antigens. J Control Release 2012;161:10-17

110. Matsuo K, Hirobe S, Yokota Y, et al. Transcutaneous immunization using a dissolving microneedle array protects against tetanus, diphtheria, malaria, and influenza. J Control Release 2012;160:495-501

- **Efficacy against various antigens of dissolving microneedles.**

111. Glenn GM, Rao M, Matyas GR, et al. Skin immunization made possible by cholera toxin. Nature 1998;391:851

112. Tierney R, Beignon AS, Rappuoli R, et al. Transcutaneous immunization with tetanus toxoid and mutants of Escherichia coli heat-labile enterotoxin as adjuvants elicits strong protective antibody responses. J Infect Dis 2003;188:753-8

113. Beignon AS, Briand JP, Muller S, et al. Immunization onto bare skin with synthetic peptides: immunomodulation with a CpG-containing oligodeoxynucleotide and effective priming of influenza virus-specific CD4+ T cells. Immunology 2002;105:204-12

114. Ozaki T, Yauchi M, Xin KQ, et al. Cross-reactive protection against influenza A virus by a topically applied DNA vaccine encoding M gene with adjuvant. Viral Immunol 2005;18:373-80

115. Kahlon R, Hu Y, Orteu CH, et al. Optimization of epicutaneous immunization for the induction of CTL. Vaccine 2003;21:2890-9

116. Anjuere F, George-Chandy A, Audant F, et al. Transcutaneous immunization with cholera toxin B subunit adjuvant suppresses IgE antibody responses via selective induction of Th1 immune responses. J Immunol 2003;170:1586-92

117. Medzhitov R, Preston-Hurlburt P, Janeway CA Jr. A human homologue of the Drosophila Toll protein signals activation of adaptive immunity. Nature 1997;388:394-7

118. Manning BM, Enioutina EY, Visic DM, et al. CpG DNA functions as an effective adjuvant for the induction of immune responses in aged mice. Exp Gerontol 2001;37:107-26

119. Seya T, Akazawa T, Tsujita T, et al. Role of Toll-like receptors in adjuvant-augmented immune therapies. Evid Based Complement Alternat Med 2006;3:31-8.discussion 133-137

120. Thissen MR, Kuijpers DI, Krekels GA. Local immune modulator (imiquimod 5% cream) as adjuvant treatment after incomplete Mohs micrographic surgery for large, mixed type basal cell carcinoma: a report of 3 cases. J Drugs Dermatol 2006;5:461-4

121. Johnston D, Bystryn JC. Topical imiquimod is a potent adjuvant to a weakly-immunogenic protein prototype vaccine. Vaccine 2006;24:1958-65

122. Zhu J, Lai K, Brownile R, et al. Porcine TLR8 and TLR7 are both activated by a selective TLR7 ligand, imiquimod. Mol Immunol 2008;45:3238-43

123. Combadiere B, Liard C. Transcutaneous and intradermal vaccination. Hum Vaccin 2011;7:811-27

124. Kim YC, Park JH, Prausnitz MR. Microneedles for drug and vaccine delivery. Adv Drug Deliv Rev 2012;64:1547-68

RIGHTSLINK

125. van der Maaden K, Jiskoot W, Bouwstra J. Microneedle technologies for (trans)dermal drug and vaccine delivery. J Control Release 2012;161:645-55

126. Celli S, Albert ML, Bousso P. Visualizing the innate and adaptive immune responses underlying allograft rejection by two-photon microscopy. Nat Med 2011;17:744-9

127. Ouchi T, Kubo A, Yokouchi M, et al. Langerhans cell antigen capture through tight junctions confers preemptive immunity in experimental staphylococcal scalded skin syndrome. J Exp Med 2011;208:2607-13

Affiliation

Sachiko Hirobe[1], Naoki Okada[†2] PhD & Shinsaku Nakagawa[*3] PhD
[†,*]Authors for correspondence
[1]Assistant Professor,
Osaka University,
Graduate School of Pharmaceutical Sciences,
Laboratory of Biotechnology and Therapeutics,
1-6 Yamadaoka, Suita, Osaka 565-0871, Japan
[2]Associate Professor,
Osaka University,
Graduate School of Pharmaceutical Sciences,
Laboratory of Biotechnology and Therapeutics,
1-6 Yamadaoka, Suita, Osaka 565-0871, Japan
Tel: +81 6 6879 8176;
Fax: +81 6 6879 8176;
E-mail: okada@phs.osaka-u.ac.jp
[3]Professor,
Osaka University,
Graduate School of Pharmaceutical Sciences,
Laboratory of Biotechnology and Therapeutics,
1-6 Yamadaoka, Suita, Osaka 565-0871, Japan
Tel: +81 6 6879 8175;
Fax: +81 6 6879 8179;
E-mail: nakagawa@phs.osaka-u.ac.jp

RIGHTSLINK

International Journal of Pharmaceutics 441 (2013) 570–579

Contents lists available at SciVerse ScienceDirect

International Journal of Pharmaceutics

journal homepage: www.elsevier.com/locate/ijpharm

Performance and characteristics evaluation of a sodium hyaluronate-based microneedle patch for a transcutaneous drug delivery system

Yasuhiro Hiraishi[a], Takeshi Nakagawa[a], Ying-Shu Quan[b], Fumio Kamiyama[b], Sachiko Hirobe[a], Naoki Okada[a,**], Shinsaku Nakagawa[a,*]

[a] Laboratory of Biotechnology and Therapeutics, Graduate School of Pharmaceutical Sciences, Osaka University, 1-6 Yamadaoka, Suita, Osaka 565-0871, Japan
[b] CosMED Pharmaceutical Co. Ltd., 32 Higashikujokawanishi-cho, Minami-ku, Kyoto 601-8014, Japan

ARTICLE INFO

Article history:
Received 29 August 2012
Received in revised form 9 October 2012
Accepted 30 October 2012
Available online 5 November 2012

Keywords:
MicroHyala®
Microneedle patch
Transcutaneous drug delivery
All-trans retinoic acid

ABSTRACT

The MicroHyala® microneedle (MN) patch was developed to provide a simple, safe, and effective drug delivery system. In this study, we examined the performance and characteristics of our fabricated MN patch to identify potential quality issues with future commercial application. Mechanical failure force analysis identified that the strength of the MN patch was affected by environmental humidity, because higher moisture levels weakened the strength of the MN. Incorporation of all-trans retinoic acid (ATRA) or ovalbumin (OVA) into the MN patch decreased the mechanical failure force by almost 50% of the strength of placebo (without drug) patches. ATRA-loaded MN patches displayed good stability after storage at 4 °C, with more than 90% and 85% of the drug remaining in the patch after 8 and 24 weeks of storage, respectively. Tetanus toxoid- and diphtheria toxoid-loaded MN patches stored for 12 months induced robust antigen-specific immune responses similar to the responses by freshly prepared MN patches. Fluorescence imaging findings suggested that prolonged antigen deposition was induced by MN-mediated fluorescein isothiocyanate-labeled (FITC)–OVA vaccination. Overall, although the strength of MN requires improvement, our developed MN patch appears to be an effective pharmaceutical product providing a simple, safe, and relatively painless approach.

© 2012 Elsevier B.V. All rights reserved.

1. Introduction

Transdermal drug delivery is an attractive administration option for small-molecule and macromolecule products, including vaccines, because of its accessibility, safety, painless drug administration, potential for self-administration, and avoidance of enzymatic degradation in the gastrointestinal tract or liver. However, the physical barrier of the stratum corneum, the outer layer of the skin, causes poor permeability across the skin and limits the bioavailability of macromolecules, thus limiting the progress of transdermal administration (Arora et al., 2008; Prausnitz, 2004; Prausnitz and Langer, 2008). To overcome this limitation, microneedle (MN) patches consisting of micron-scale needles assembled on a transdermal patch have been developed using fabrication technology of the microelectronics industry (Kim et al., 2012a; Prausnitz et al., 2009).

Although MN technology was first developed in the early 1970s, few studies demonstrated the its usefulness as a tool for transdermal drug delivery, until the advancement of microelectronics technology in the 1990s. MN fabrication technology has rapidly progressed since then. MNs have been made from silicon, metal, or polymer (Kim et al., 2012a; Kis et al., 2012). The majority of research papers published thus far used nondissolving MNs. Metal-based MNs coated with water-soluble formulations facilitate the successful delivery of agents such as insulin (Gill and Prausnitz, 2007), salmon calcitonin (Tas et al., 2012), parathyroid hormone (PTH; 1–34) (Ameri et al., 2010), hepatitis B surface antigen (Andrianov et al., 2009), inactivated influenza virus (Zhu et al., 2009), influenza virus-like particle (Quan et al., 2010), bacillus Calmette–Guérin (Hiraishi et al., 2011), and influenza virus hemagglutinin-DNA (Kim et al., 2012b; Song et al., 2012) into the skin.

Polymer MNs that dissolve in the skin have also been developed recently; these MNs display successful delivery and efficacy (Sullivan et al., 2010). Compared with metal-based MNs, polymer-based dissolving MNs have several potential advantages. Because polymer-based MNs dissolve completely in the skin, they cannot be

Abbreviations: MN, microneedle; ATRA, all-trans retinoic acid; TT, tetanus toxoid; DT, diphtheria toxoid; OV, ovalbumin; FITC–OVA, fluorescein isothiocyanate-labeled ovalbumin; HPLC, high-performance liquid chromatography; ERH, equilibrium relative humidity; ID, intradermal; PBS, phosphate-buffered saline; HSD, honestly significant difference; ANOVA, analysis of variance.

* Corresponding author. Tel.: +81 6 6879 8175; fax: +81 6 6879 8179.
** Corresponding author. Tel.: +81 6 6879 8176; fax: +81 6 6879 8176.
E-mail addresses: okada@phs.osaka-u.ac.jp (N. Okada), nakagawa@phs.osaka-u.ac.jp (S. Nakagawa).

0378-5173/$ – see front matter © 2012 Elsevier B.V. All rights reserved.
http://dx.doi.org/10.1016/j.ijpharm.2012.10.042

intentionally reused, which may help prevent the transmission of blood-borne pathogens and diseases caused by reuse of needle and syringes in developing countries. In addition, they can completely eliminate biohazardous sharp waste after use and safety concerns such as fractured metal needles piercing the skin (Al-Zahrani et al., 2012).

In our earlier studies, we developed a sodium hyaluronate-based dissolving MN patch called MicroHyala®. Sodium hyaluronate is a component of skin tissue and is hydrophilic in nature; thus, it may be biocompatible with the skin and safe for exogenous material insertion, which has been verified by our recent study involving healthy human volunteers (submitted for publication). We also demonstrated that transcutaneous immunization using the MN patch induces immune responses against ovalbumin (OVA), adenoviral vectors, tetanus, diphtheria, malaria, and influenza, with comparable efficacy to traditional hypodermic needle-based immunization (Matsuo et al., 2012a,b). These safety and efficacy findings indicate that our developed MN patch is a promising delivery system. Considering its future commercial application, there are several critical attributes necessary for product quality. First, MNs need to be precisely inserted into the skin without mechanical failure in order to ensure drug delivery into the skin, which requires sufficient MN strength (Lee et al., 2008). Second, MNs should dissolve in the skin's interstitial fluid within no more than a few hours (hopefully within a few minutes) to minimize the patch application time; a shorter application time may be better from the point of view of patient compliance. Third, the stability of the drug loaded into the MN patch is an important factor for efficacy. Furthermore, thermostable vaccine formulations could facilitate increased vaccine coverage, especially in developing countries that lack an adequate healthcare infrastructure for cold-chain storage (Bell et al., 2001; Berhane et al., 2000).

In the present study, we investigated the performance and characteristics of a sodium hyaluronate-based MN patch. We evaluated the mechanical failure force of MNs and the dissolution characteristics of drugs from MNs. In addition, the stability performance of drug-loaded MN patches was assessed using all-trans retinoic acid (ATRA; vitamin A acid) and the tetanus toxoid (TT)/diphtheria toxoid (DT) divalent vaccine as model compounds. We also described the deposition of antigen in mouse skin by in vivo fluorescence imaging after MN administration using comparisons with traditional hypodermic needle-based intradermal (ID) administration.

2. Materials and methods

2.1. Animals

Six-week-old female Wistar–ST rats and 7- to 10-week-old female ICR mice were purchased from Japan SLC Inc. (Hamamatsu, Japan). Seven- to nine-week-old female HR-1 hairless mice were purchased from SHIMIZU Laboratory Supplies Co., Ltd. (Kyoto, Japan). All animals were housed at the Osaka University animal facility. All animal studies were conducted in accordance with the guidelines provided by the Animal Care and Use Committee of Osaka University.

2.2. Fabrication of the dissolving MN patch

As described previously (Matsuo et al., 2012b), the dissolving MN patch was fabricated at CosMED Pharmaceutical Co. Ltd., (Kyoto, Japan) using micromolding technologies with sodium hyaluronate as the base material. Previously developed MN contained collagen. In this study, we used a collagen-free MH as collagen is suspected to induce inflammation in human. In brief, sodium hyaluronate (JP grade, Kikoman Biochemifa Company, Tokyo, Japan), dextran 70 (JP grade, Meito Sangyo, Nagoya, Aichi), and Polyvidone (JPE grade, BASF Japan, Tokyo, Japan) were dissolved in distilled water at a ratio of 11:8:1 and then mixed with ATRA (Sigma–Aldrich Inc., St. Louis, MO, USA), OVA (Sigma–Aldrich Inc.), fluorescein isothiocyanate-labeled–OVA (FITC–OVA; Molecular Probes, Eugene, OR, USA), or the TT/DT divalent vaccine (The Research Foundation for Microbial Diseases of Osaka University, Suita, Japan). The aqueous solution was casted onto micromolds and then dried in a desiccator at room temperature. The dissolving MN patches were obtained by removing them from the micromolds. Placebo dissolving MN patches were also fabricated in the same manner, without an active pharmaceutical ingredient. The MN patches contained more than 200 MNs/cm^2. To form the MN transcutaneous patch system, patches with an area of 0.8 cm^2 were fixed onto an adhesive film with a surface area of 2.3 cm^2. Hence, our dissolving MN patch system consisted of the MicroHyala® patch with MNs that were 200 (MH200), 300 (MH300), or 800 μm (MH800) in length.

2.3. Moisture conditioning and moisture content measurement of the MN patch

To condition the MN patch to different moisture contents, the patch was placed in desiccators containing Tri-Sorb molecular sieves (Süd-Chemie Performance Packaging, Colton, CA, USA) or a saturated solution of potassium acetate (Wako Pure Chemical, Osaka, Japan), magnesium chloride hexahydrate (Wako Pure Chemical), potassium carbonate (Wako Pure Chemical), or sodium chloride (Wako Pure Chemical). The desiccators were stored at room temperature (25 °C) for 1 week in an environment of 0, 22, 33, 44, or 75% relative humidity (RH) (Young, 1967). After removal of the MN patch from the desiccator, the endpoint moisture level was evaluated as a function of equilibrium relative humidity (ERH) using a water activity analyzer (HygroLab; Rotronic AG, Bassersdorf, Switzerland).

2.4. Measurement of mechanical failure force for MNs

The force necessary for mechanical MN fracture was measured using a TA-XT plus texture analyzer (StableMicro Systems, Surrey, UK). An MN patch was attached to a test station by double-sided adhesive tape. Axial force was then applied using a flathead 5-mm diameter stainless steel cylinder to move the cylinder at a rate of 0.6 and 1.1 mm/min for MH300 and MH800, respectively, and the trigger force was set at 0.049 N.

2.5. Quantification of ATRA loaded into the MN patch

To determine the amount of ATRA loaded into the MN patches, MNs were first removed from the base material using a razor. The removed MNs were soaked in distilled water followed by vortex mixing to completely dissolve them. Ethanol (Wako Pure Chemical) was added to the sample solution followed by vortex mixing, and the sample solution was then diluted with acetonitrile (Wako Pure Chemical). The sample solution was filtered through a membrane filter (0.45-μm diameter) and analyzed using a high-performance liquid chromatography (HPLC) method, as reported previously (Tashtoush et al., 2007). In brief, a D-2000 Elite HPLC system (Hitachi, Tokyo, Japan) was used. Chromatographic separation was performed using a reverse-phase Nucleosil 5 μm C18 100A column (250 mm × 4.6 mm; GL Science Inc., Tokyo, Japan). The mobile phase comprised 0.01% trifluoroacetic acid and acetonitrile (15:85, v/v) at a flow rate of 1 ml/min. The column temperature was 40 °C, and the detection wavelength was 342 nm. The concentration of ATRA in the sample solution was determined using a standard curve

based on known concentrations of ATRA, which was converted to the absolute mass of ATRA loaded into the MN patch with a dilution factor. The ATRA MN patch was packaged in a heat-sealed aluminum laminated sachet under a refrigerated condition (4 °C) or at room temperature (25 °C) to examine the shelf-life.

2.6. Dissolution of ATRA from MNs and delivery to skin

MNs were imaged by brightfield stereomicroscopy (VHX-1000; Keyence Corporation, Osaka, Japan). To prevent moisture uptake by environmental humidity that may affect needle failure force and dissolution characteristics, MN patches were packed in moisture impermeable package, heat-sealed aluminum laminated sachet, before use, and used for the study immediately after opening the package. The back skin of the HR-1 hairless mice was pierced with the ATRA-loaded MN patch (MH800) using a handheld applicator (Matsuo et al., 2012b) under isoflurane inhalation anesthesia. The patch was left in place for 30, 60, or 120 min and covered with a wound management film (BIOCLUSIVE; Johnson & Johnson Medical, Ltd., Tokyo, Japan). After removing the patch, the efficiency of drug delivery into the skin was determined by comparing (i) the residual amount of ATRA on the MN patch after skin insertion, (ii) the amount of ATRA deposited onto the skin surface, and (iii) the amount initially loaded. The amount of ATRA deposited onto the skin surface was evaluated by applying adhesive tape (Scotch tape, 3M, St. Paul, MN, USA) to the skin surface; immersing the tape in distilled water, ethanol, and acetonitrile (6:4:90, v/v); and determining the amount of ATRA by HPLC. Using a mass balance, the amount of ATRA delivered into the skin was determined by subtracting the amount remaining on the MN patch and on the skin surface after insertion from the amount originally on the noninserted MN patch.

2.7. Fluorescence imaging for antigen deposition assessment

Hair on the back of the ICR mice was shaved using clippers and completely removed using a depilatory lotion (Kracie, Tokyo, Japan) under isoflurane inhalation anesthesia. This hair removal protocol is frequently employed in our laboratory for MN vaccination studies and is similar to procedures used in the literature (Hiraishi et al., 2011). The FITC–OVA (1 μg protein)-loaded MN patch was administered. The patch was pressed into the skin using a handheld applicator and left in place for 60 min covered with a wound management film. After removal of the patch, the skin was harvested, frozen in OCT compound (Sakura Finetechnical Co., Ltd., Tokyo, Japan), and cut into 8-μm-thick sections using a cryostat. Histological examination of the skin was performed on frozen sections that were mounted with Prolong Gold antifade reagent with DAPI (Invitrogen, Carlsbad, CA) and then photographed using fluorescence microscopy (BZ-8000; Keyence Corporation, Osaka, Japan).

To perform in vivo fluorescence imaging, the HR-1 hairless mice were treated with an FITC–OVA (10 μg protein)-loaded MN patch (MH300), ID injection of phosphate-buffered saline (PBS) containing FITC–OVA (10 μg protein/30 μl), or ID injection of FITC–OVA (10 μg protein/30 μl) that was removed from the MN patch and reconstituted by ID injection in PBS on the back skin under isoflurane inhalation anesthesia. The reconstituted solution consisted of 10 μg FITC–OVA, 386 μg sodium hyaluronate, 284 μg dextran 70, and 36 μg polyvidone in 30 μl PBS. Fluorescence images were obtained using the CRi Maestro EX in vivo imaging system (Cambridge Research and Instrumentation, Woburn, MA). To capture the FITC image, a blue filter for excitation at 455 nm and a blue emission filter at 515 nm were used. The exposure time was 200 ms, and spectral resolution for all imaging was 10 nm. Measurements of integrated fluorescence intensity for the injection site were made by Maestro version 2.10 software.

2.8. Vaccination and ELISA assay for IgG

To evaluate the stability of the hyaluronate-based MN patch, combined TT (20 μg) and DT (10 μg)-loaded MN patches (MH800) were stored at 4, 25, or 40 °C for up to 12 months before vaccination. Hair on the back of the Wistar–ST rats was removed using clippers and a depilatory lotion. The stored MN patch was pressed into the skin using a handheld applicator under isoflurane anesthesia, covered with a wound management film, and left in place for 6 h. The freshly prepared MN patches were also administered as a comparable vaccination. Vaccinations were repeated 5 times every 2 weeks. At the indicated periods, sera were collected from the rats to determine the antigen-specific IgG titers by ELISA according to previously described protocols (Matsuo et al., 2011). The endpoint titers of antigen-specific antibodies were expressed as the reciprocal $\log_2$ of the last dilution that had an absorbance value of 0.1 absorbance units after subtracting the background.

2.9. Challenge study for tetanus toxin

For the challenge study, the rats vaccinated with stored MN patches were subcutaneously injected in the hind leg with a lethal dose (1 μg) of tetanus toxin (Sigma–Aldrich, Inc.) 1 month after the final vaccination. The rats were observed daily for 4 days to record mortality.

2.10. Statistical analysis

The data obtained were analyzed by Student's *t*-test, Tukey–Kramer's honestly significant difference (HSD) test, or analysis of variance (ANOVA) using JMP software ver. 8.0 (SAS Institute Inc., Cary, NC, USA). In all cases, $p < 0.05$ was considered significant.

3. Results

3.1. Fabrication of the MN patch and investigation of mechanical failure force

MN patches fabricated using micromolding technologies were designed to be sufficiently long to penetrate across the stratum corneum barrier and into the skin but sufficiently short to prevent pain (Gill et al., 2008). The MNs used in this study were 200 (MH200), 300 (MH300), or 800 μm (MH800) in length.

To assure drug delivery into the skin, MNs need to be precisely inserted into the skin without mechanical failure. The mechanical failure force of MNs was assessed according to a previously described method (Park et al., 2005). A force displacement curve revealed that force initially increased with the displacement of the stainless steel cylinder pressed against MNs, followed by a sudden decline in force, which was interpreted as the point of MN failure (Fig. 1A). After the failure force test, MNs were evaluated by brightfield stereoscopic microscopy (Fig. 1B).

Because of the hygroscopic nature of sodium hyaluronate, our fabricated MN patch may easily absorb moisture after exposure to high humidity, which may affect needle strength. We first conditioned MN patches to various humidity conditions, obtaining MN patches with different moisture levels. The moisture level of the MN patch was assessed as the water activity of ERH (Heidemann and Jarosz, 1991). After 1 week of storage in a desiccator, the moisture levels changed relative to the storage humidity (Fig. 2A). The water activity of the MN patch before storage was 18.5%, and this increased to 59.1% after storage at 75% RH for 1 week. We next

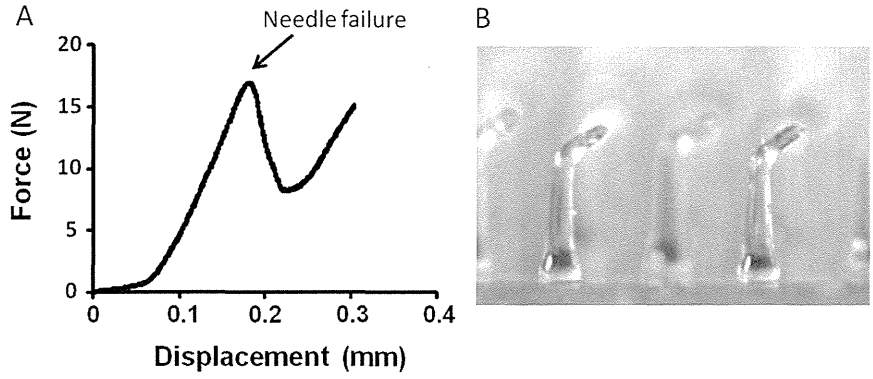

Fig. 1. Mechanical failure force analysis of microneedles (MNs). Force was measured as a function of the displacement of the stainless steel cylinder pressed against the MNs. (A) Representative failure behavior of MNs under an axial load. Needle failure was identified by a sudden drop in force. (B) Brightfield stereomicrograph of MNs after an axial failure test.

measured the mechanical failure force of MNs using the moisture-conditioned MN patches (Fig. 2B). Data are presented as the force per needle required for failure using a needle density and the flat surface area of the stainless steel cylinder for axial loading. The mechanical failure force was dependent on the moisture level of the MN patch (ANOVA, $p < 0.01$). When the water activity of the patch was 59.1%, the failure force was 0.14 N per needle, which was nearly 50% lower than that of a dried MN patch (18.5% water activity after storage at 0% RH).

To better understand the influence of active pharmaceutical ingredients on needle strength, ATRA and OVA were selected as our model small molecule and macromolecule compounds, respectively, and loaded into MN patches. The failure forces of ATRA MNs were less than 0.1 N per needle, with ranges of 0.04–0.056 N for MH300 (Fig. 3A) and 0.073–0.1 N for MH800 (Fig. 3B). Compared with the failure force of placebo MNs (Fig. 2B), the failure force was decreased by approximately 50% on incorporation of ATRA. The amount of ATRA in the MN patch did not affect the failure force at the amounts evaluated (ANOVA, $p > 0.05$). Similarly, the failure forces of OVA MNs (Fig. 3C, D) were lower than those of placebo MNs, irrespective of the amount of OVA loaded (ANOVA, $p > 0.05$).

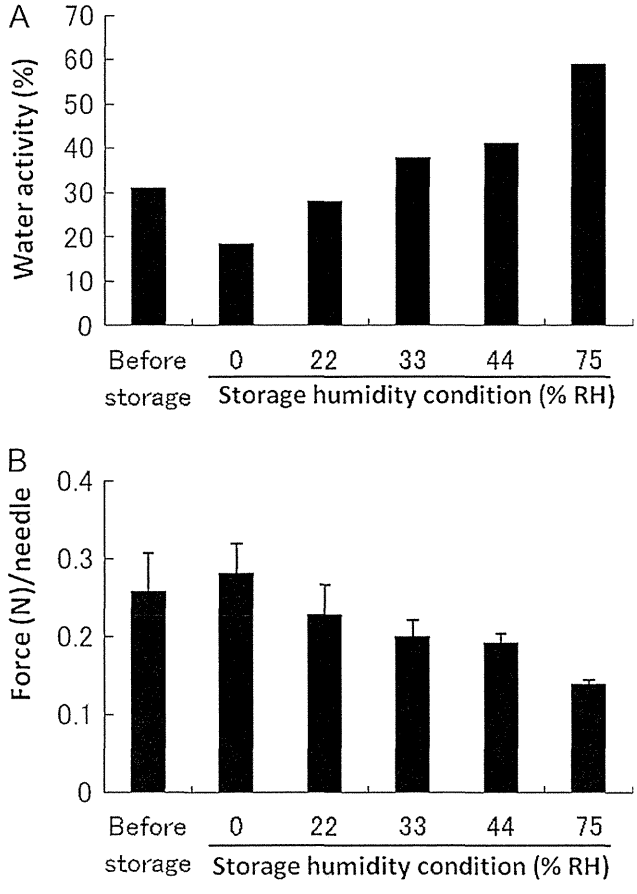

Fig. 2. Water activity and mechanical failure force for placebo MNs. (A) Water activity of MH800 after storage under various humidity conditions. The water activity was measured using a water activity analyzer. As a control, the water activity before storage was also measured. (B) Mechanical failure force of MH800 as a function of water activity. The force required to fracture 55 MNs was measured using a TA-XT plus texture analyzer. Data represent the average ± standard deviation of 3 measurements each.

3.2. Dissolution characteristics of MNs

In our previously published studies, we demonstrated that placebo MNs completely dissolved in 60 min after insertion into mouse or rat skin (Matsuo et al., 2012b). In this study, we selected ATRA as a model compound to evaluate the dissolution characteristics of drug-loaded MNs. Because of the poor water solubility of ATRA (Didja et al., 1989), we considered it a good model compound for evaluating the dissolution capability of our fabricated MNs for comparisons with placebo or water-soluble compound-loaded MNs.

Brightfield micrographs of ATRA MNs before and after insertion demonstrated that the MNs were almost completely dissolved 120 min after application (Fig. 4A). To better understand the degree of ATRA delivery, the amount of ATRA delivered into the skin was measured using HPLC by subtracting the amount of drug remaining in the MN patch and on the skin surface after insertion from the amount originally loaded into the noninserted MN patch. After insertion into the skin for 120 min, almost all the ATRA was released into the skin at a delivery rate exceeding 90% (Fig. 4B). However, 60 min of application was not sufficient for complete delivery (76% delivery rate), and the needle bottom remained on the base material (Fig. 4A).

3.3. Localization and deposition of antigen delivered by the MN patch

To monitor the delivery of antigen into the skin, the mice were administered FITC–OVA as a model antigen. Fig. 5 represents histological sections of the insertion site in mouse skin after insertion of the MNs for various application times. The resulting needle track crossed the epidermis and into the superficial dermis and revealed that antigen was delivered (green spot) to both of these layers. With

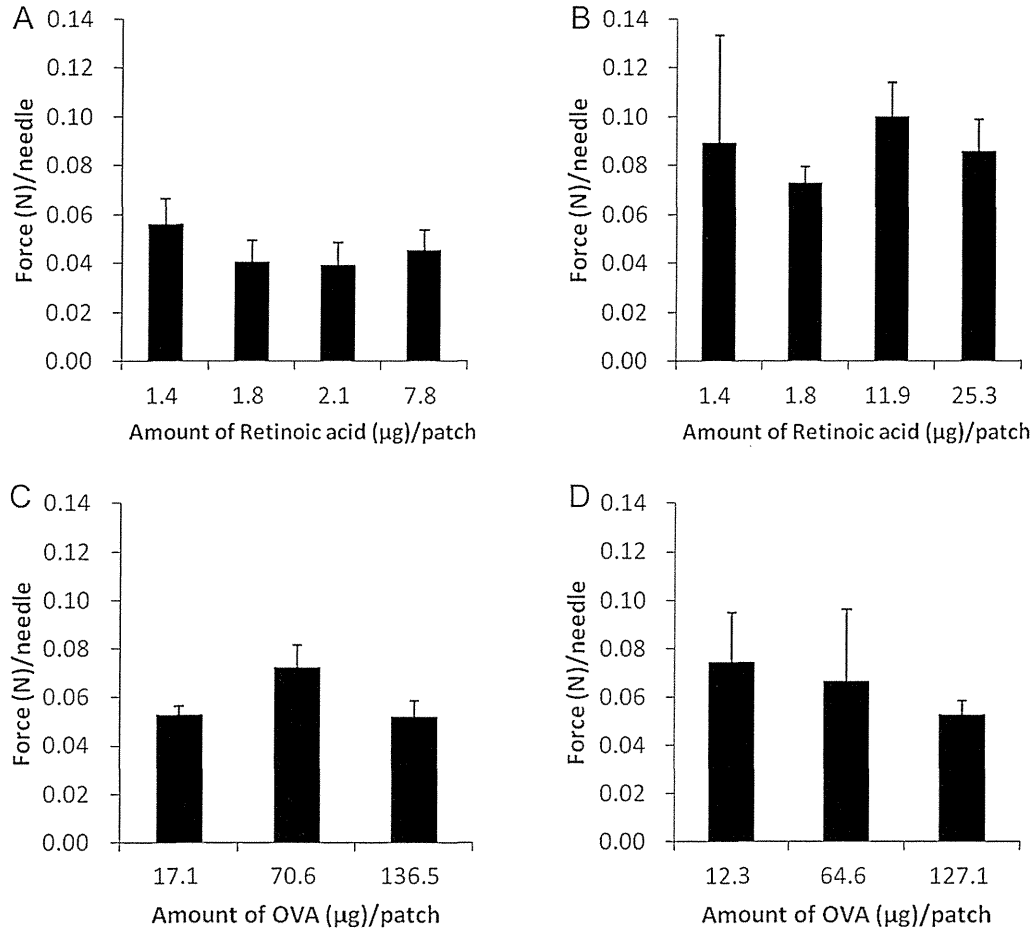

Fig. 3. Mechanical failure force for MNs as a function of the amount of drug loaded. (A) All-trans retinoic acid (ATRA)-loaded MH300, (B) ATRA-loaded MH800, (C) ovalbumin (OVA)-loaded MH300, and (D) OVA-loaded MH800. Data represent the average ± standard deviation of 3 measurements each.

a 3-h application time, antigen remained around the insertion site. With longer application times, the antigen gradually diffused in the superficial dermis.

We next monitored the deposition of antigen in vivo after administration of FITC–OVA into mouse skin using the FITC–OVA-loaded MN patch by drawing comparisons between ID immunization using an FITC–OVA PBS solution or reconstituted FITC–OVA solution obtained from the MN patch using a 26-gauge hypodermic needle. Fluorescence micrographs demonstrated that the amount of antigen injected by the ID method reduced drastically 3 h after administration, whereas a slight green spot remained up to 47 and 24 h when the reconstituted solution and PBS solution were injected intradermally, respectively (Fig. 6A). In contrast, intense antigen deposition corresponding to the administration site of the MN patch was observed up to 47 h after administration, and a small green spot remained after 74 h. Fig. 6B shows the kinetics of the integrated fluorescence intensity for the injection site, which indicated that MN patch administration resulted in prolonged antigen deposition compared with other administration methods.

3.4. Stability performance of the MN patch

ATRA is known to be chemically unstable. When ATRA is exposed to light, heat, or oxidants, it is rapidly degraded into isomerized products (Brisaert et al., 1995; Lim et al., 2004). To evaluate the stability performance of our sodium hyaluronate-based MN patch and its possible shelf-life, we selected ATRA as a model compound. ATRA MN patches packaged in heat-sealed aluminum laminated sachets were stored in a refrigerated condition (4 °C) for 3 different manufacturing lots or at room temperature (25 °C) for 1 lot. The amount of ATRA in the MN patch was assayed by HPLC and expressed as the percentage of the initial (without storage) amount (Fig. 7). The amount of ATRA in the patch was significantly reduced after storage at room temperature (25 °C) for 1 week (78.1 ± 11.6%, Student's t-test, $p < 0.05$), and continued storage up to 24 weeks resulted in additional loss of ATRA to 44.8 ± 23.3% (Student's t-test, $p < 0.05$). Conversely, there was no significant loss of ATRA under the refrigerated condition (4 °C) for 24 weeks (86.1 ± 5.4%, Student's t-test, $p = 0.08$), and all 3 lots exhibited similar trends for stability during refrigerated storage.

We next used the combined TT/DT-loaded patches in an additional stability assessment. The vaccination efficacies of antigen-specific IgG titers were evaluated as a stability characteristic indicator. The vaccination protocol and animal model (rat) were those of previously reported methods (Matsuo et al., 2012a). The TT/DT-loaded MN patches were exposed to various storage conditions and then administered into the exposed back skin of rats. After 6 months of storage at 4, 25, or 40 °C in heat-sealed aluminum laminated sachets, both anti-TT and anti-DT IgG titers increased with increasing numbers of vaccinations (Fig. 8A, B). Continued storage for up to 12 months at the same temperatures (Fig. 8C, D) followed by vaccination also resulted in the induction of pronounced antigen-specific IgG levels comparable with those induced by freshly prepared MN patches (Tukey–Kramer HSD, $p > 0.05$). Furthermore, the storage temperature did not affect the immune response induced by loaded TT (20 μg) and DT (10 μg) (ANOVA,

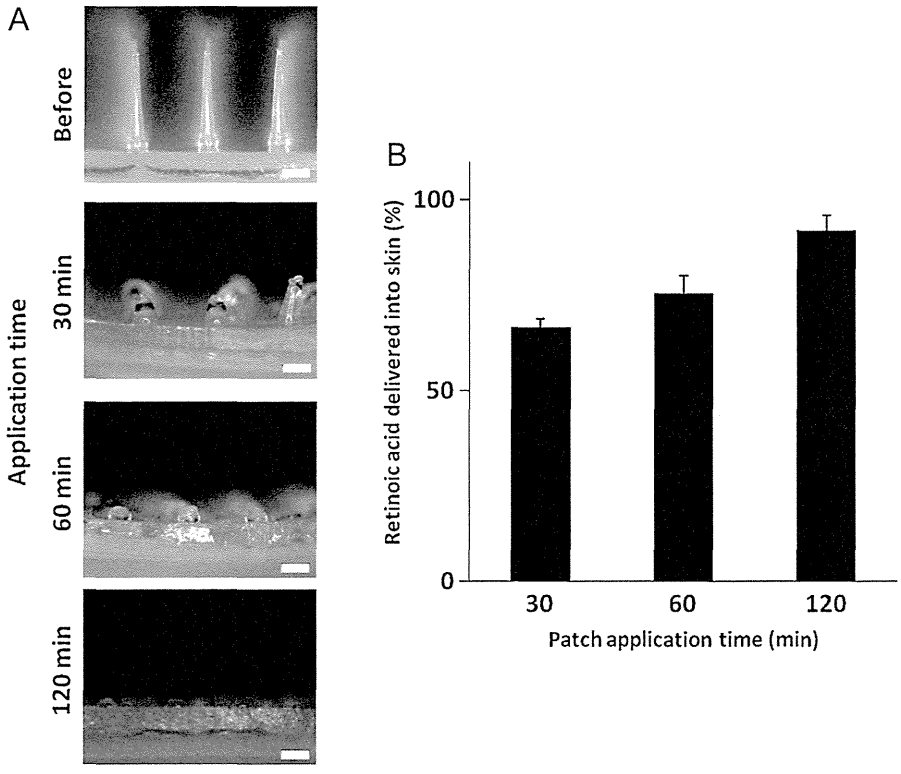

Fig. 4. Dissolution of ATRA-loaded MNs. (A) Stereoscopic micrographs of MNs (scale bar, 200 μm). The MN patches were pressed into the back skin of HR-1 hairless mice and left for 30, 60, or 120 min. After 120 min, almost all the MNs were dissolved. (B) Percentage of ATRA delivered into the skin as a function of the application time.

$p > 0.05$). Although further investigation is necessary with lower antigen amounts and different animal species, these results support that our MN patch was highly immunogenic in rats even after long-term storage for 12 months.

To ensure the immunogenicity of the stored MN patch, we conducted a challenge study. The rats vaccinated with the stored MN patches were injected with a lethal dose of 1 μg tetanus toxin 1 month after the final vaccination. The nonvaccination group was not included in this study because of animal care guidelines. The rats were observed daily for 4 days to record mortality. The data illustrated that all animals vaccinated using the stored MN patches survived the tetanus toxin challenge (Table 1).

4. Discussion

Over the past 15 years, the field of MN technology has rapidly progressed, with more than 350 research papers being published. Many pharmaceutical companies have entered this field. The Soluvia® microinjection system consisting of short, hollow, steel needles is now available for vaccination (Kim et al., 2012a). The metal-based MN patch from ZOSANO has moved into a Phase II clinical trial for the administration of PTH (1–34) for treating osteoporosis (Cosman et al., 2010). With regard to dissolving polymer MN patches, to our knowledge, no commercially available products are yet available in the pharmaceutical field. Our MicroHyala® patch is the only dissolving MN patch available; it has only been used for cosmetic products. For further exploration of our patch in the pharmaceutical field, we have been investigating the possibility of its application in vaccination. We have demonstrated its effectiveness with various antigens (Matsuo et al., 2012a,b). As a next step, we are investigating the possibility of commercial application. Commercial products require several attributes to assure their quality, such as dissolution of a drug from the MN patch and identification of the degradation products. Assays of content uniformity, needle strength, aseptic integrity, and stability performance will be required for the MN patch. In this study, as an initial step to assess these attributes, we evaluated the needle strength, dissolution characteristics, and stability of the patch using model compounds. Furthermore, the therapeutic use of ATRA as a dermatological treatment (Darlenski et al., 2010), antitumor agent (Ozpolat and Lopez-Berestein, 2002; Zuccari et al., 2005), and immunomodulator (Skountzou et al., 2006) motivated us to evaluate the feasibility of ATRA MN patches.

Our MicroHyala® patch is composed of sodium hyaluronate as a base material. Sodium hyaluronate may be biocompatible as it is a skin tissue component that is hydrophilic in nature. This will be advantageous for safety. However, its hydrophilic nature may adversely affect needle strength when the MN patch is exposed to environmental humidity, and this could be a critical issue for usage and storage in high humidity environments, especially in *WHO Climatic Zone IV* countries (Kopp, 2006). The mechanical failure force test results indicated that the needle strength decreased as the moisture level of the MN patch increased. To simulate its usage in high humidity conditions, MN patches (MH800) were stored at 55% RH and 25 °C or 95% RH and 37 °C for 30 min. Then, the patches were pressed into the back skin of ICR mice using the handheld applicator. After removal of the MN patch, the MNs remaining on the patch were examined. The MNs stored at 55% RH and 25 °C were successfully pressed on the skin of the mice, and they dissolved into the skin. In contrast, the MNs stored at 95% RH and 37 °C bent from the needle bottom, and they could not be pressed into the skin (Supplementary Fig. S1). These data suggested that the MN patch should be packaged in a moisture-impermeable container before use, and immediate use after opening a package is recommended. Facilitating increased vaccination coverage, especially in developing countries lacking adequate healthcare infrastructures, requires further improvement in the strength of the needle to improve its stability in high humidity by optimizing the base components. For optimization of base material, we plan to perform a material screening using a moisture sorption isotherm for a material,

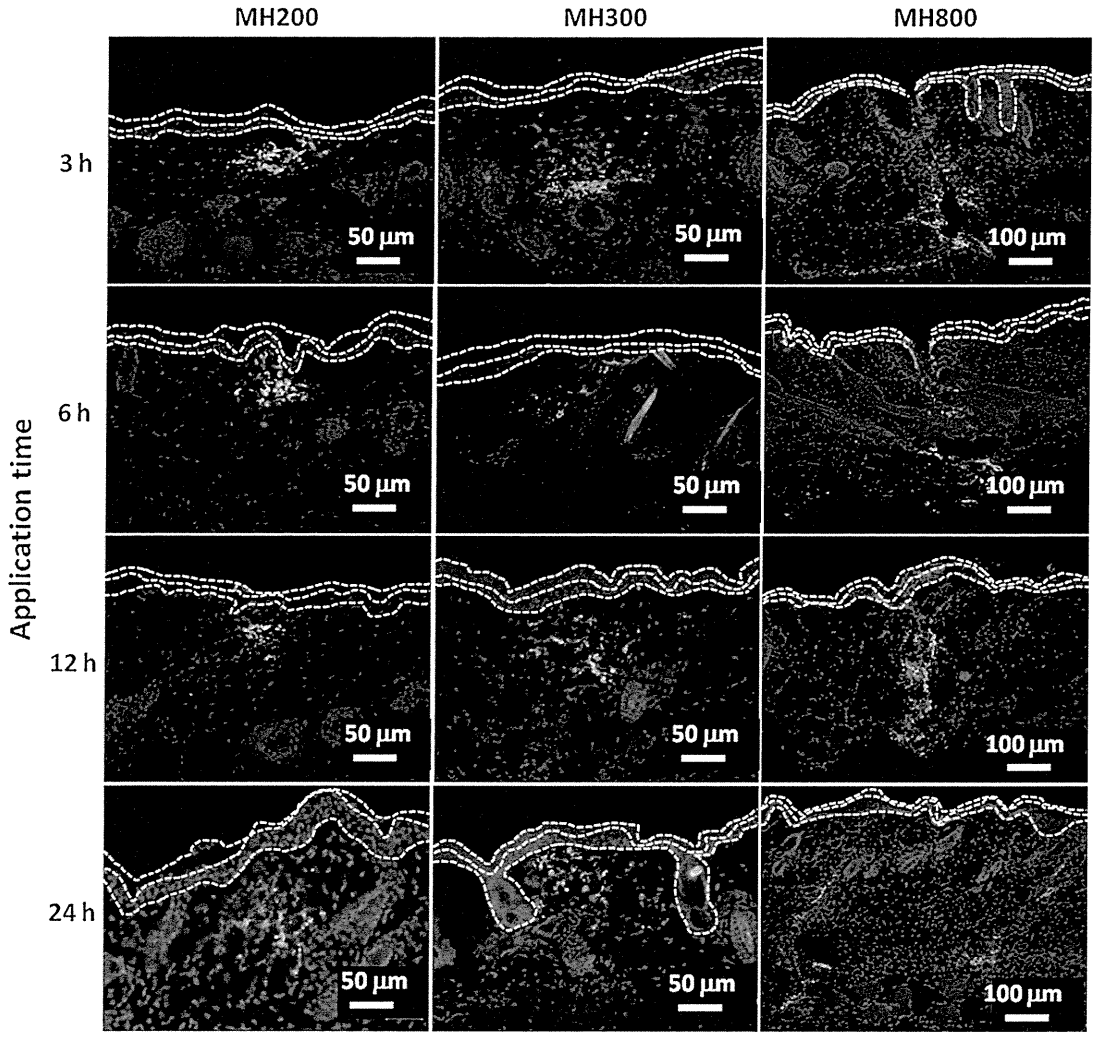

Fig. 5. Histological section of the back skin of ICR mice treated with fluorescein isothiocyanate-labeled (FITC)–OVA-loaded MH200, MH300, or MH800 for 3, 6, 12, or 24 h. After removal of the MN patch, the skin was harvested and frozen. Frozen sections (8-μm-thick) were photographed using a fluorescence microscope. The resulting needle track crossed the epidermis and into the superficial dermis, revealing that FITC–OVA was delivered (green spot) to both these layers. The nucleus was counterstained using DAPI (blue). The white dotted lines indicate the surfaces of the stratum corneum, epidermis, and superficial dermis, respectively, from top to bottom.

which is the relationship between water content and equilibrium humidity of a material. Preferable material for dissolving MNs need to show low moisture content at the environmental humidity of 11–75%RH to keep sufficient needle strength, and high moisture content at high humidity of more than 90%RH to dissolve quickly. We currently consider adding a disaccharide as an improvement option.

We also found that incorporating ATRA or OVA decreases the needle strength compared with the strength of placebo MNs (no active pharmaceutical ingredient). According to a previous report, the insertion force required for MNs with a tip diameter of 25 μm to pierce the skin is 0.058 N per needle (Park et al., 2005). Our fabricated MN has a tip diameter of 30 μm, which may require a similar insertion force as that reported by Park et al. For a sufficient safety margin for skin insertion by application of gentle force by the thumb, the needle strength must exceed 0.058 N per needle. However, the needle strength of ATRA- or OVA-loaded MNs was less than 0.1 N per needle (Fig. 3). In this study, there was

Table 1
Rat tetanus toxin challenge study.

Vaccination[a]			Tetanus toxin (μg)[b]	Survival ratio (survival rat/tested rat)
Storage condition	Method	TT (μg)		
4 °C for 6 months	MNs	20	1	5/5
25 °C for 6 months	MNs	20	1	5/5
40 °C for 6 months	MNs	20	1	5/5
4 °C for 12 months	MNs	20	1	5/5
25 °C for 12 months	MNs	20	1	5/5
40 °C for 12 months	MNs	20	1	5/5

[a] Vaccinations were repeated 5 times every 2 weeks.
[b] Tetanus toxin (1 μg) was subcutaneously injected in the hind leg.

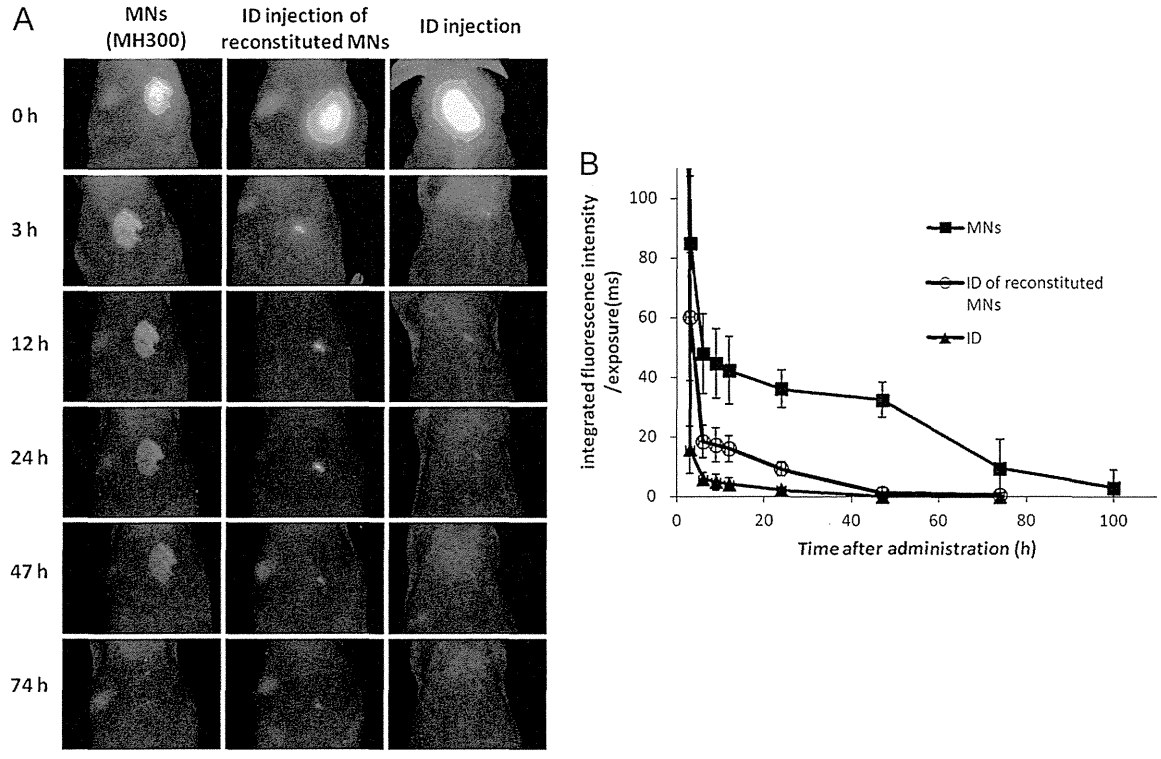

Fig. 6. Kinetics of antigen deposition after FITC–OVA administration to HR-1 hairless mice via MN patch delivery, intradermal (ID) injection of reconstituted FITC–OVA, or ID injection of phosphate-buffered saline containing FITC–OVA. (A) Representative in vivo fluorescence imaging for antigen deposition from 4 mice for each group. Images were captured by the CRi Maestro EX system at the indicated time point after administration. Here, time 0 means the time of MN removal after 1-h application. (B) Integrated fluorescence intensity for the injection site as a function of time after administration. The intensity was measured from images captured using Maestro version 2.10 software. Data represent the average ± standard deviation of 4 measurements each.

no sufficient margin for safety, which resulted in the use of an applicator for insertion. In commercial use, rapid mass vaccination and self-administration require robust needle strength to enable administration without special training or equipment. Thus, we believe that further improvement in needle strength is necessary.

Dissolution characteristics evaluation using ATRA MN patches provided a better understanding of the application time. Placebo or OVA MNs were sufficiently dissolved within 60 min (Matsuo et al., 2012b). ATRA MNs required a 120-min application time for sufficient dissolution. This longer application time may be because of the poor water solubility of ATRA. For further evaluation of dissolution characteristics, antigen diffusion and deposition were assessed using FITC–OVA. FITC–OVA administration using MN patches resulted in prolonged antigen deposition compared with ID administration via a hypodermic needle. Prolonged antigen deposition via MN patch administration might depend on the greater viscosity of sodium hyaluronate than of the PBS solution. These observations are similar to the results of del Pilar Martin et al., that is, stainless steel MN vaccination of a Qdot-labeled influenza virus also resulted in prolonged antigen deposition in the skin for up to 7 days (del Pilar Martin et al., 2012), and they suggested that the prolonged deposition might be because of the large size of the inactivated virus antigen and the kinetics of antigen trafficking to the draining lymph nodes. In addition to roles as an immune stimulant, aluminum hydroxide adjuvant also contributes to antigen deposition. These findings will be a potential advantage of MN immunization; that is, prolonged antigen exposure to antigen-presenting cells leads to robust immune responses.

Chemical stability data revealed that ATRA MN patches packaged in heat-sealed aluminum laminated sachet are stable under refrigerated conditions (4 °C) for up to 24 weeks. It is well known that ATRA is not stable against light, heat, or oxidants. Various

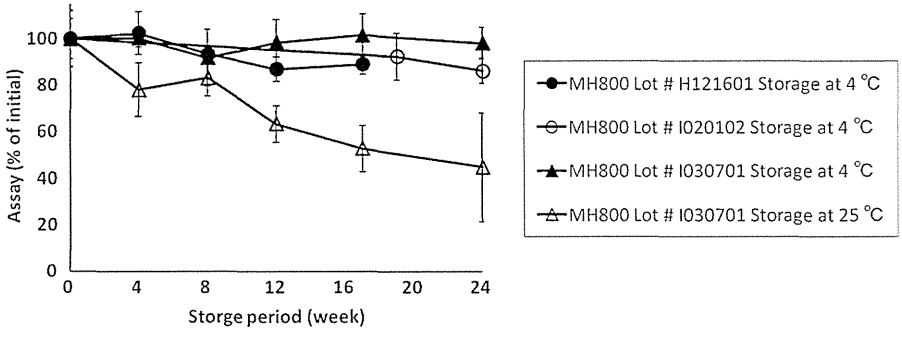

Fig. 7. ATRA stability as a function of storage time at 4 or 25 °C for ATRA-loaded MN patches. ATRA content was assayed by high-performance liquid chromatography. Data represent the average ± standard deviation of 4 measurements each. Almost 15% drug loss was observed after storage at 4 °C for 24 weeks, but this loss was not significant (Student's *t*-test, $p = 0.08$). Conversely, approximately 50% loss was observed after 24 weeks at 25 °C (Student's *t*-test, $p < 0.05$).

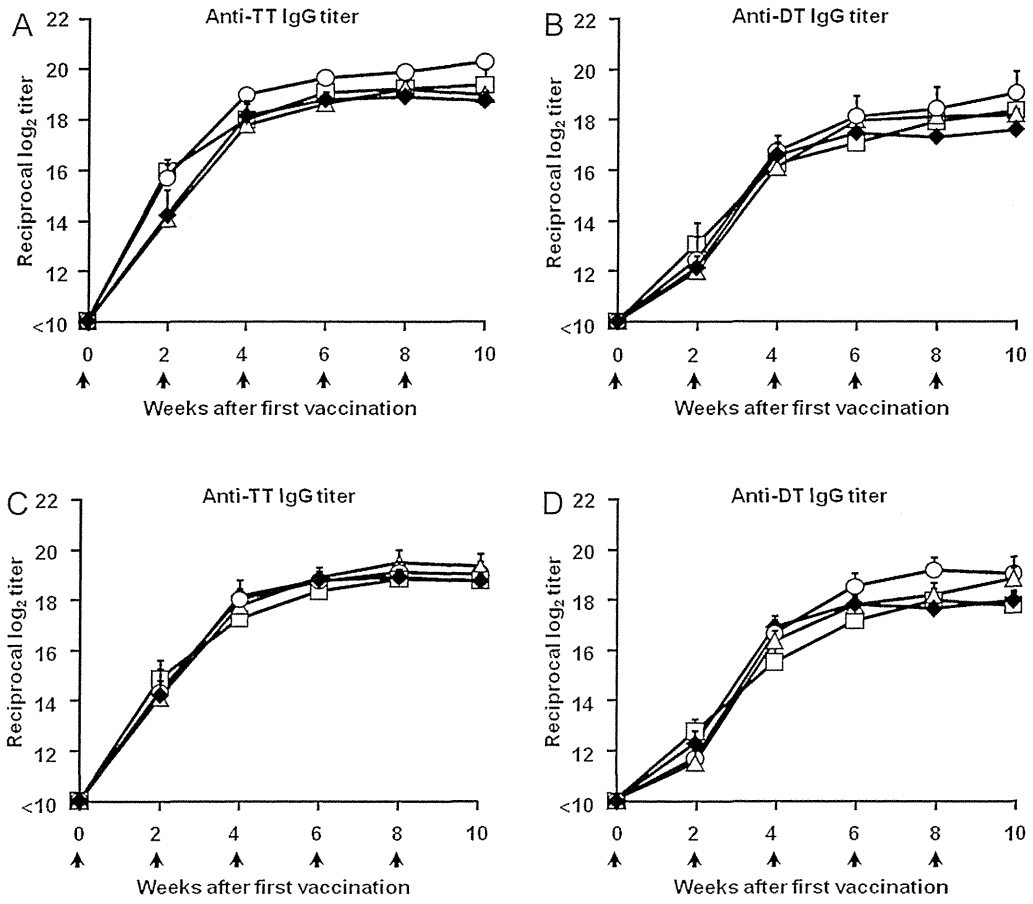

Fig. 8. Antigen-specific antibody responses after vaccination using MN patches (MH800) stored at various temperatures for 6 or 12 months. Combined tetanus toxoid (TT; 20 μg) and diphtheria toxoid (DT; 10 μg)-loaded MN patches stored at 4, (○), 25 °C (□), 40 °C (Δ) for (A) (B) 6 or (C–D) 12 months were pressed into the back skin of Wistar–ST rats. Vaccinations were repeated 5 times every 2 weeks. Arrows indicate the vaccination timing. As a control, freshly prepared combined TT (20 μg) and DT (10 μg)-loaded MN patches were also pressed into the back skin of Wistar–ST rats under the same vaccination schedule (♦). At the indicated periods, sera were collected from the rats to determine the toxoid-specific IgG titers. Data are expressed as mean ± standard error of 5 measurements.

formulations have been investigated (Brisaert et al., 1995; Hattori et al., 2012; Ozpolat and Lopez-Berestein, 2002; Zuccari et al., 2005). Lim et al. developed a solid lipid nanoparticle formulation to improve the stability, which exhibited good stability with more than 90% of the drug remaining after 1 month of storage at 4 °C. Our formulated ATRA MN patch also exhibited good stability after storage at 4 °C, with more than 90 and 85% of the drug remaining after 8 and 24 weeks of storage, respectively. The results indicated no significant incompatibility of the drug with the component materials of MicroHyala®, sodium hyaluronate, dextran 70, and polyvidone. Because of the many therapeutic applications of ATRA, particularly in dermatological treatment, successful fabrication of ATRA MN patches allowed us to extend MN technology to both vaccination and novel therapeutic development in dermatology. As a proof of principle, we plan to investigate the feasibility of ATRA MN patches in the treatment of seborrheic keratosis, a common skin tumor.

Our study also demonstrated that MN patches stored at 40 °C for 12 months could induce robust antigen-specific immune responses comparable with those induced by freshly prepared MNs (Fig. 8). In addition to the immune response, the dissolution kinetics of TT/DT-loaded MNs was not changed by storage (Supplementary Fig. S2). Although further investigations using lower doses of vaccines or different types of vaccines are needed, the thermostabilities confirmed in this study suggest that MN vaccine formulations could be stored at room temperature, which would be an important benefit to increase vaccination coverage in developing countries where refrigeration is not sufficient.

5. Conclusion

This study evaluated the performance and characteristics of sodium hyaluronate-based MN patches to identify potential quality issues for future commercial usage. The advantage of prolonged antigen deposition after MN vaccination would lead to superior immune responses compared with those of traditional hypodermic needle vaccination. In addition, good stability without significant incompatibility with ATRA and TT/DT vaccines would permit the production of thermostable products. The ATRA MN patch will facilitate the development of new dermatological therapeutic applications. Overall, although its needle strength needs to be improved, our transcutaneous drug delivery system utilizing MicroHyala® would be an effective product for the simple, safe, and relatively painless delivery of drugs.

Acknowledgments

We acknowledge the Research Foundation for Microbial Diseases of Osaka University (Suita, Japan) for providing TT and DT, Kazuyuki Niki at Osaka University for help with the animal studies, and Tomomi Sato at Osaka University for assistance with fluorescence imaging by the CRi Maestro EX system. This work was supported by the Advanced Research for Medical Products Mining Programme of the National Institute of Biomedical Innovation (NIBIO); by Health and Labour Sciences Research Grants in Research on New Drug Development from the Ministry of Health, Labour, and Welfare; and by a Grant-in-Aid for Scientific Research (B)

(24390041) from the Ministry of Education, Culture, Sports, Science, and Technology of Japan.

Appendix A. Supplementary data

Supplementary data associated with this article can be found, in the online version, at http://dx.doi.org/10.1016/j.ijpharm.2012.10.042.

References

Al-Zahrani, S., Zaric, M., McCrudden, C., Scott, C., Kissenpfennig, A., Donnelly, R.F., 2012. Microneedle-mediated vaccine delivery: harnessing cutaneous immunobiology to improve efficacy. Expert Opin. Drug Deliv. 9, 541–550.

Ameri, M., Fan, S., Maa, Y.-F., 2010. Parathyroid hormone PTH(1-34) formulation that enables uniform coating on a novel transdermal microprojection delivery system. Pharm. Res. 27, 303–313.

Andrianov, A.K., DeCollibus, D.P., Gillis, H.A., Kha, H.H., Marin, A., Prausnitz, M.R., Babiuk, L.A., Townsend, H., Mutwiri, G., 2009. Poly[di(carboxylatophenoxy)phosphazene] is a potent adjuvant for intradermal immunization. Proc. Natl. Acad. Sci. U.S.A. 106, 18936–18941.

Arora, A., Prausnitz, M.R., Mitragotri, S., 2008. Micro-scale devices for transdermal drug delivery. Int. J. Pharm. 364, 227–236.

Bell, K.N., Hogue, C.J.R., Manning, C., Kendal, A.P., 2001. Risk factors for improper vaccine storage and handling in private provider offices. Pediatrics 107, e100.

Berhane, Y., Demissie, M., 2000. Cold chain status at immunisation centres in Ethiopia. East Afr. Med. J. 77, 476–479.

Brisaert, M.G., Everaerts, I., Plaizier-Vercammen, J.A., 1995. Chemical stability of tretinoin in dermatological preparations. Pharm. Acta Helv. 70, 161–166.

Cosman, F., Lane, N.E., Bolognese, M.A., Zanchetta, J.R., Garcia-Hernandez, P.A., Sees, K., Matriano, J.A., Gaumer, K., Daddona, P.E., 2010. Effect of transdermal teriparatide administration on bone mineral density in postmenopausal women. J. Clin. Endocrinol. Metab. 95, 151–158.

Darlenski, R., Surber, C., Fluhr, J.W., 2010. Topical retinoids in the management of photodamaged skin: from theory to evidence-based practical approach. Br. J. Dermatol. 163, 1157–1165.

del Pilar Martin, M., Weldon, W.C., Zarnitsyn, V.G., Koutsonanos, D.G., Akbari, H., Skountzou, I., Jacob, J., Prausnitz, M.R., Compans, R.W., 2012. Local response to microneedle-based influenza immunization in the skin. MBio 3 (2), http://dx.doi.org/10.1128/mBio.00012-12, e00012–12.

Didja, A., Darrouzet, H., Duchêne, D., Poelman, M.-C., 1989. Inclusion of retinoic acid in β-cyclodextrin. Int. J. Pharm. 54, 175–179.

Gill, H.S., Denson, D.D., Burris, B.A., Prausnitz, M.R., 2008. Effect of microneedle design on pain in human volunteers. Clin. J. Pain 24, 585–594, 510.1097/AJP.1090b1013e31816778f31816779.

Gill, H.S., Prausnitz, M.R., 2007. Coating formulations for microneedles. Pharm. Res. 24, 1369–1380.

Hattori, M., Shimizu, K., Katsumura, K., Oku, H., Sano, Y., Matsumoto, K., Yamaguchi, Y., Ikeda, T., 2012. Effects of all-trans retinoic acid nanoparticles on corneal epithelial wound healing. Graefes Arch. Clin. Exp. Ophthalmol. 250, 557–563.

Heidemann, D., Jarosz, P., 1991. Preformulation studies involving moisture uptake in solid dosage forms. Pharm. Res. 8, 292–297.

Hiraishi, Y., Nandakumar, S., Choi, S.-O., Lee, J.W., Kim, Y.-C., Posey, J.E., Sable, S.B., Prausnitz, M.R., 2011. Bacillus Calmette–Guérin vaccination using a microneedle patch. Vaccine 29, 2626–2636.

Kim, Y.-C., Park, J.-H., Prausnitz, M.R., 2012a. Microneedles for drug and vaccine delivery. Adv. Drug Deliv. Rev., http://dx.doi.org/10.1016/j.addr.2012.04.005.

Kim, Y.C., Song, J.M., Lipatov, A.S., Choi, S.O., Lee, J.W., Donis, R.O., Compans, R.W., Kang, S.M., Prausnitz, M.R., 2012b. Increased immunogenicity of avian influenza DNA vaccine delivered to the skin using a microneedle patch. Eur. J. Pharm. Biopharm. 81, 239–247.

Kis, E.E., Winter, G., Myschik, J., 2012. Devices for intradermal vaccination. Vaccine 30, 523–538.

Kopp, S., 2006. Stability testing of pharmaceutical products in a global environment. RAJ Pharma http://apps.who.int/medicinedocs/en/m/abstract/Js19134en/

Lee, J.W., Park, J.H., Prausnitz, M.R., 2008. Dissolving microneedles for transdermal drug delivery. Biomaterials 29, 2113–2124.

Lim, S.-J., Lee, M.-K., Kim, C.-K., 2004. Altered chemical and biological activities of all-trans retinoic acid incorporated in solid lipid nanoparticle powders. J. Control. Release 100, 53–61.

Matsuo, K., Hirobe, S., Yokota, Y., Ayabe, Y., Seto, M., Quan, Y.-S., Kamiyama, F., Tougan, T., Horii, T., Mukai, Y., Okada, N., Nakagawa, S., 2012a. Transcutaneous immunization using a dissolving microneedle array protects against tetanus, diphtheria, malaria, and influenza. J. Control. Release 160, 495–501.

Matsuo, K., Ishii, Y., Quan, Y.-S., Kamiyama, F., Mukai, Y., Yoshioka, Y., Okada, N., Nakagawa, S., 2011. Transcutaneous vaccination using a hydrogel patch induces effective immune responses to tetanus and diphtheria toxoid in hairless rat. J. Control. Release 149, 15–20.

Matsuo, K., Yokota, Y., Zhai, Y., Quan, Y.-S., Kamiyama, F., Mukai, Y., Okada, N., Nakagawa, S., 2012b. A low-invasive and effective transcutaneous immunization system using a novel dissolving microneedle array for soluble and particulate antigens. J. Control. Release 161, 10–17.

Ozpolat, B., Lopez-Berestein, G., 2002. Liposomal-all-trans-retinoic acid in treatment of acute promyelocytic leukemia. Leuk. Lymphoma 43, 933–941.

Park, J.H., Allen, M.G., Prausnitz, M.R., 2005. Biodegradable polymer microneedles: fabrication, mechanics and transdermal drug delivery. J. Control. Release 104, 51–66.

Prausnitz, M.R., 2004. Microneedles for transdermal drug delivery. Adv. Drug Deliv. Rev. 56, 581–587.

Prausnitz, M.R., Langer, R., 2008. Transdermal drug delivery. Nat. Biotechnol. 26, 1261–1268.

Prausnitz, M.R., Mikszta, J.A., Cormier, M., Andrianov, A.K., 2009. Microneedle-based vaccines. Curr. Top. Microbiol. Immunol. 333, 369–393.

Quan, F.S., Kim, Y.C., Vunnava, A., Yoo, D.G., Song, J.M., Prausnitz, M.R., Compans, R.W., Kang, S.M., 2010. Intradermal vaccination with influenza virus-like particles by using microneedles induces protection superior to that with intramuscular immunization. J. Virol. 84, 7760–7769.

Skountzou, I., Quan, F.-S., Jacob, J., Compans, R.W., Kang, S.-M., 2006. Transcutaneous immunization with inactivated influenza virus induces protective immune responses. Vaccine 24, 6110–6119.

Song, J.-M., Kim, Y.-C.O.E., Compans, R.W., Prausnitz, M.R., Kang, S.-M., 2012. DNA vaccination in the skin using microneedles improves protection against influenza. Mol. Ther. 20, 1472–1480.

Sullivan, S.P., Koutsonanos, D.G., Del Pilar Martin, M., Lee, J.W., Zarnitsyn, V., Choi, S.O., Murthy, N., Compans, R.W., Skountzou, I., Prausnitz, M.R., 2010. Dissolving polymer microneedle patches for influenza vaccination. Nat. Med. 16, 915–920.

Tas, C., Mansoor, S., Kalluri, H., Zarnitsyn, V.G., Choi, S.-O., Banga, A.K., Prausnitz, M.R., 2012. Delivery of salmon calcitonin using a microneedle patch. Int. J. Pharm. 423, 257–263.

Tashtoush, B.M., Jacobson, E.L., Jacobson, M.K., 2007. A rapid HPLC method for simultaneous determination of tretinoin and isotretinoin in dermatological formulations. J. Pharm. Biomed. Anal. 43, 859–864.

Young, J.F., 1967. Humidity control in the laboratory using salt solutions—a review. J. Appl. Chem. 17, 241–245.

Zhu, Q.Y., Zarnitsyn, V.G., Ye, L., Wen, Z.Y., Gao, Y.L., Pan, L., Skountzou, I., Gill, H.S., Prausnitz, M.R., Yang, C.L., Compans, R.W., 2009. Immunization by vaccine-coated microneedle arrays protects against lethal influenza virus challenge. Proc. Natl. Acad. Sci. U.S.A. 106, 7968–7973.

Zuccari, G., Carosio, R., Fini, A., Montaldo, P.G., Orienti, I., 2005. Modified polyvinylalcohol for encapsulation of all-trans-retinoic acid in polymeric micelles. J. Control. Release 103, 369–380.

Supplementary Figures

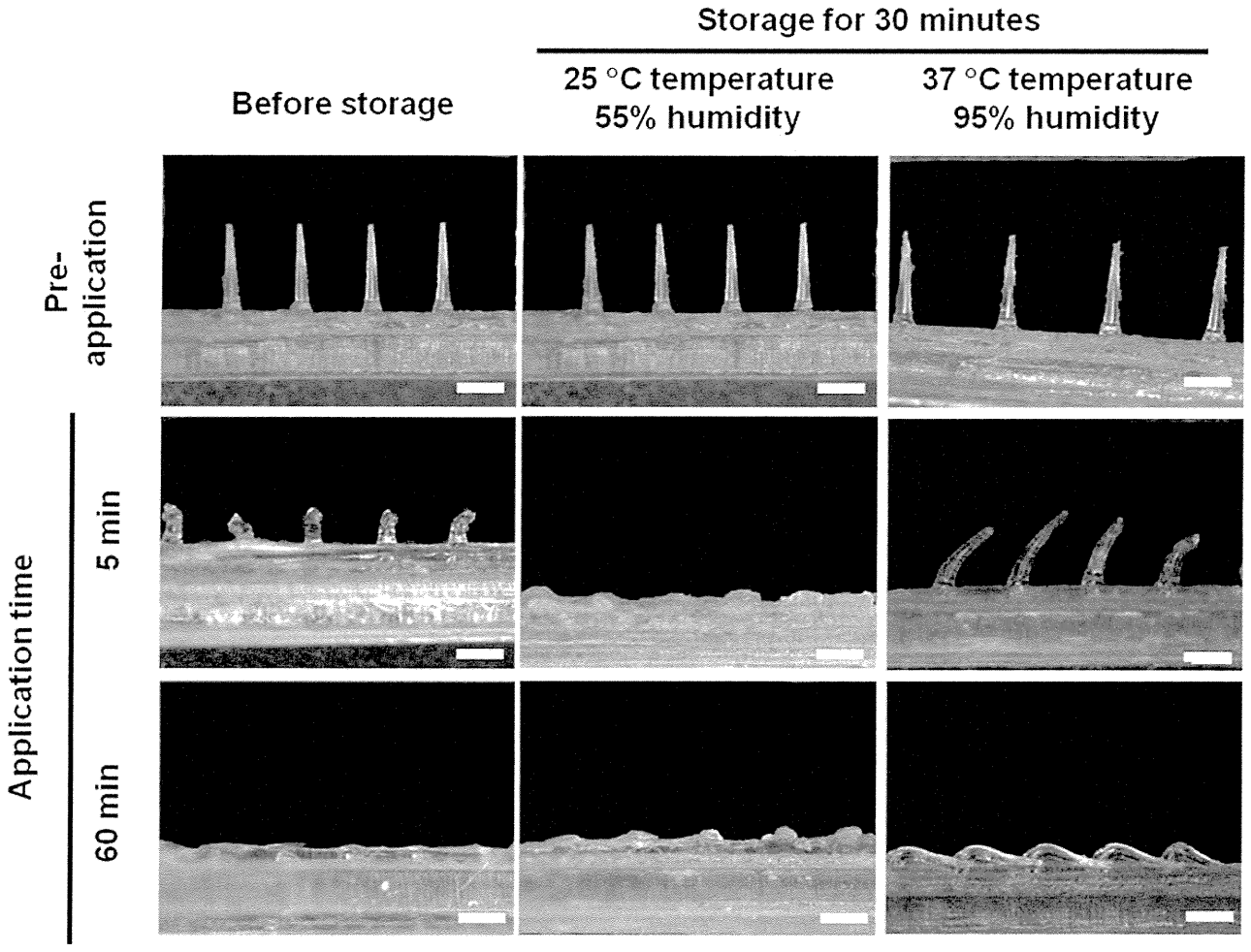

Fig. S1: Dissolution kinetics of placebo MNs before and after 30 min of storage in various conditions. MN patches (MH800) were stored at 55% RH and 25 °C or at 95% RH and 37 °C for 30 min. Then, the MN patches were pressed into the back skin of ICR mice for 5 or 60 min. After removal of the MN patch, the MNs remaining on the skin were photographed using a stereoscopic microscope (scale bar, 300 μm).

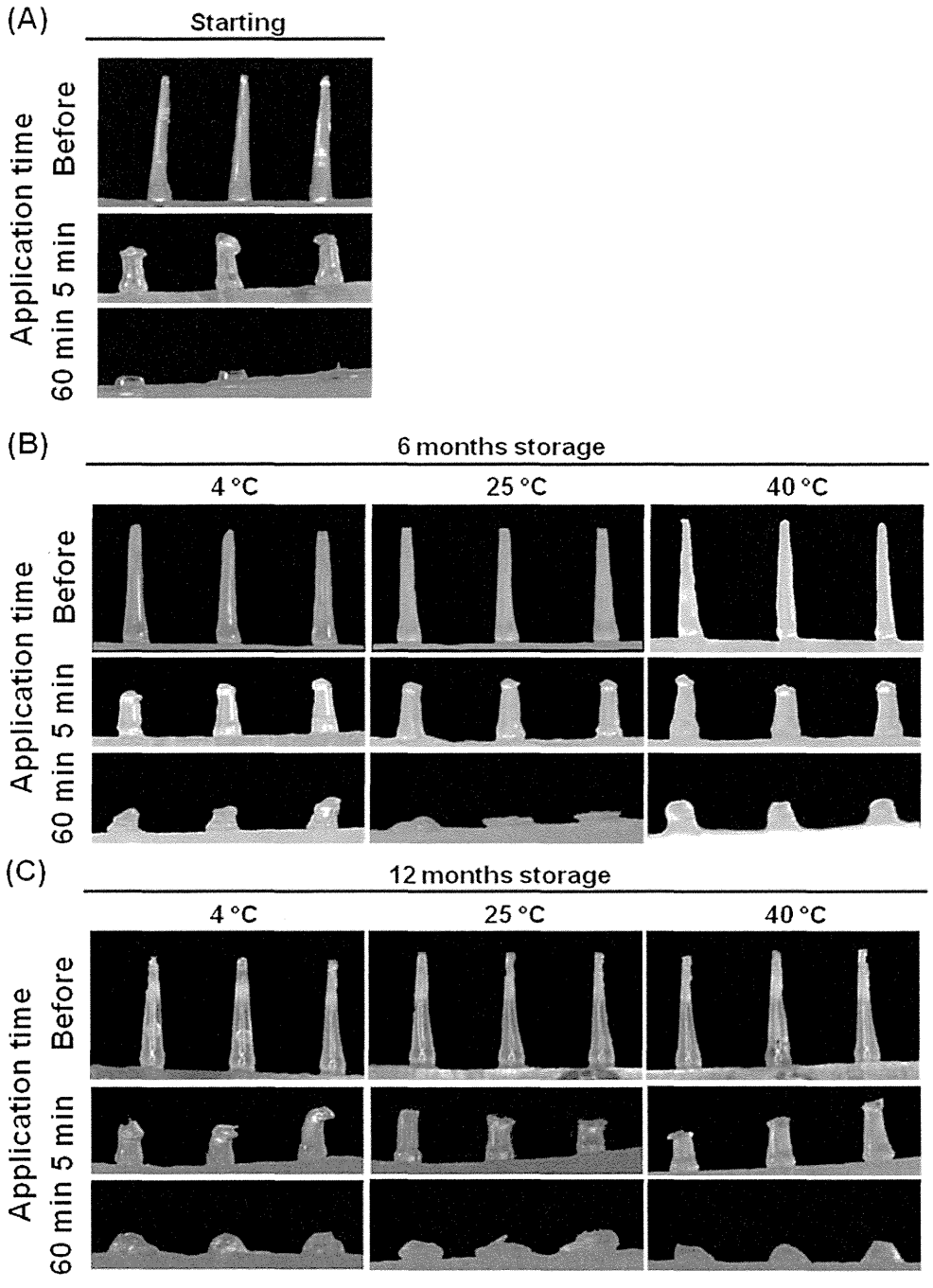

Fig. S2: Dissolution kinetics of combined TT/DT vaccine-loaded MNs (A) before storage or after storage at 4, 25, or 40 °C for (B) 6 or (C) 12 months. The MN patches (MH800) were pressed into the back skin of Wistar–ST rats and left for 5 or 60 min. After removal of the patch, the MNs remaining on the skin were photographed using a stereoscopic microscope.

—Symposium Review—

経皮ワクチン製剤（貼るワクチン）の基礎から臨床

岡田直貴

From Basic Principles to Clinical Applications on Transcutaneous Vaccine

Naoki Okada

Laboratory of Biotechnology and Therapeutics, Graduate School of Pharmaceutical Sciences, Osaka University; 1-6 Yamadaoka, Suita, Osaka 565-0871, Japan.

(Received August 30, 2013)

The recent vigorous transnational migration of people and materials reflecting the development of transportation facilities, changes in social structure, and war disasters has increased the global spread of emerging and re-emerging infectious diseases. Vaccine, which is the major fundamental prophylaxis against infectious diseases, has greatly contributed to the maintenance and improvement of human health worldwide. However, the disadvantages of conventional injection systems hamper the speedy mass-vaccination and the global distribution of vaccines. Transcutaneous immunization systems, which are easy-to-use and low-invasive methods of vaccination, have the potential to overcome certain issues associated with injectable vaccinations. In this review, we provide an outline of recent trends in the development of techniques for the transcutaneous delivery of vaccine antigens. We also introduce basic and clinical research involving our transcutaneous immunization systems that incorporate self-dissolving microneedle patch.

Key words——vaccine; transcutaneous immunization; microneedle; influenza

1. はじめに

人類と感染症の係わりの歴史は古く，エジプトのミイラからは天然痘に感染した痕が確認されている．ウイルスや細菌の誕生が人類の誕生以前の出来事であったことを想起すれば，人類の誕生とともに感染症との闘いの歴史が始まったといっても過言ではない．人類は感染症との長い闘いの中で，医学の進歩や公衆衛生事業の拡大により多くの戦果を得てきた．なかでもワクチンは，感染症に対する根本的予防における唯一の手段であり，疾患の発症並びに症状の重篤化を抑制する画期的な医薬品である．

ワクチン開発は1798年のEdward Jennerによる牛痘接種法（天然痘ワクチン）に始まり，200年以上の歴史を持つ．Jennerの種痘以後，細菌学，ウイルス学の発達により，感染症の原因となる病原体が次々と同定され，数多くのワクチンが開発されてきた．現在においても，新たに分子生物学的手法を駆使して，より安全で有効なワクチンの開発が進められている．しかしながら，依然として感染症は世界における死亡原因の第一位を占めており，高度に発達した交通網が様々な人的・物的交流に伴う国境を越えた病原体の移動を可能にしている．2009年のインフルエンザパンデミック騒動が記憶に新しいように，新興・再興感染症の世界規模での流行の脅威にさらされている現代社会においては，国際的な視野での感染症対策が喫緊の課題となっている．

このような社会背景の下，近年のワクチン研究領域においては，各種感染症に対するワクチンの開発・改良やワクチンを大量かつ迅速に製造・供給できる技術の開発と併せて，簡便，低侵襲，安価な新規ワクチン接種法及びワクチン剤形の開発が重要な研究課題として注目されている．これまでに実用化されたワクチンの大半は注射製剤として開発されており，接種に医療従事者を必要とする技術的な問題や，製造・輸送・保管における一貫した低温管理（cold chain）を必要とする費用的な問題が，開発途上国へのワクチン普及の大きな障壁となっている．また，注射は痛みを伴うとともに，注射針を介した二次感染の危険性や医療廃棄物の処理などの安

The author declares no conflict of interest.

大阪大学大学院薬学研究科薬剤学分野（〒565-0871 大阪府吹田市山田丘1-6)
e-mail: okada@phs.osaka-u.ac.jp

本総説は，日本薬学会第133年会シンポジウムS30-106で発表した内容を中心に記述したものである．

全面での問題も有する．さらに，感染症パンデミックやバイオテロリズム発生時におけるワクチンの迅速大規模接種に注射投与では対応できない点も懸念されている．

そこで筆者らは，簡便な予防接種を可能にする皮膚を標的とした経皮ワクチン製剤「貼るワクチン」の開発を推進しており，本稿では，経皮ワクチンデリバリー技術として近年注目されているマイクロニードル法について概説するとともに，筆者らの皮膚内溶解型マイクロニードルパッチを応用した「貼るワクチン」に関する研究成果を紹介する．

2. ワクチンの標的組織としての皮膚

皮膚は生体を外界と隔てる障壁であり，異物の侵入を防ぐ“物理的バリアー”と異物の除去を担う“免疫学的バリアー”を有する（Fig. 1）．解剖学的にみれば外側から角質層（stratum corneum; SC），生きた表皮（顆粒層，有棘層，基底層），真皮の大きく3層に分けられており，最外層のSCはケラチンタンパク質でできた角質細胞が幾重にも重なることで構成され，物理的バリアーの主役となっている．一方，角質層下の生きた表皮並びに真皮には免疫学的バリアーを構築する様々な細胞群が存在しており，なかでも生きた表皮に常在するランゲルハンス細胞（Langerhans cells; LC）と真皮に分布する真皮樹状細胞（dermal dendritic cell; dDC）は，抗原提示細胞として外来異物に対する生体防御機構において重要な役割を担っている．[1] また，生きた表皮を構成する細胞の90％以上を占めるケラチノサイト（keratinocyte; KC）は，異物の侵入を感知してサイトカイン・ケモカインなどの炎症メディエーターを産生することで自然免疫の誘導に係わる．[2] 経皮ワクチンは，これらの免疫担当細胞により形成される皮膚の免疫学的バリアーを利用する新規ワクチン手法であり，皮膚内のLCやdDCへと効率よくワクチン抗原を送達することができれば，ワクチン抗原を捕食したこれら抗原提示細胞が所属リンパ節へと遊走し，T細胞並びにB細胞を抗原特異的に活性化することで強力な免疫応答を惹起できると考えられる．

しかしながら，経皮ワクチンの開発においてワク

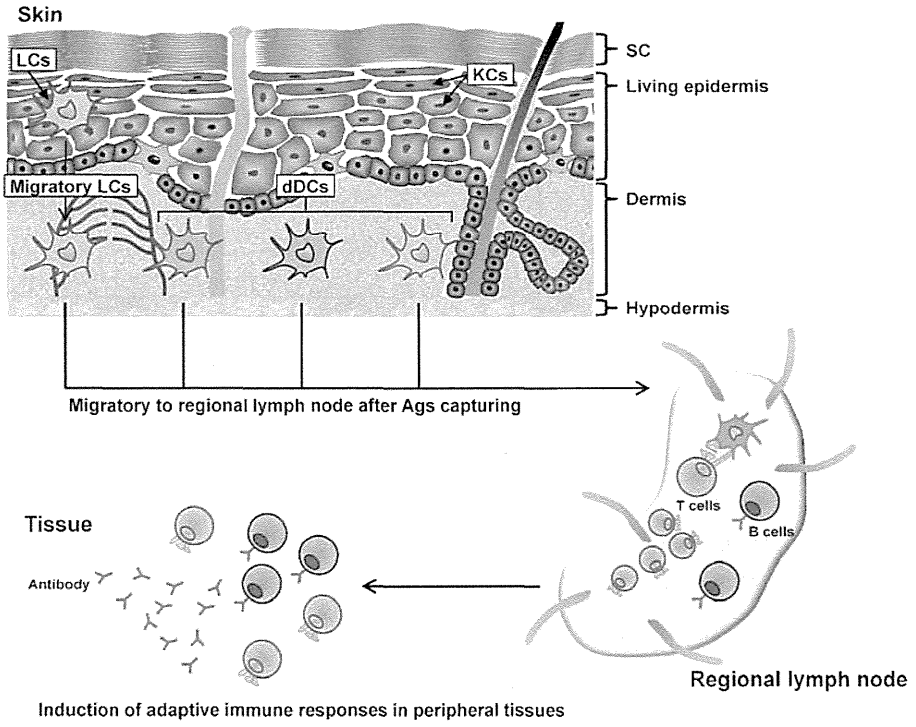

Fig. 1. Skin Immune System

The stratum corneum (SC) is the outermost of the epidermis and is largely responsible for the vital barrier function of the skin. The living epidermis and dermis under the SC are enriched with various immunocompetent cells such as Langerhans cells (LCs), keratinocytes (KCs), and several kinds of dermal dendritic cells (dDCs). KCs as principal epidermal cells are mainly involved in the induction of inflammation and innate immunity by cytokine production. LCs and dDCs capture external antigens (Ags), migrate into regional lymph nodes, present Ags to T cells, and activate Ag-specific T cells and B cells. Activated T cells and B cells distribute to peripheral tissues and demonstrate Ag-specific immune responses.

チン抗原デリバリーの障壁となるのが，前述したSCの存在である．SCはケラチンや繊維状タンパク質，さらにはセラミドや中性脂質からなり立っており，水溶性物質や分子量が500以上の物質の透過を制限している.[3] 現在実用化されているワクチンは，①弱毒化した生きたウイルスや細菌を用いる生ワクチン（BCG，麻疹ワクチンなど），②病原性をなくした病原体全体あるいは病原性に係わる免疫原を用いる不活化ワクチン（日本脳炎ワクチン，インフルエンザHAワクチンなど），③細菌が出す毒素を不活化したトキソイド（破傷風トキソイド，ジフテリアトキソイドなど），といった高分子タンパク質や粒子状のコンポーネント，細菌やウイルス自体である．したがって，ワクチン抗原を単に皮膚表面に塗布するだけでは皮膚内へと到達することができず，免疫応答を誘導することは困難である．

角質層下，主に真皮へと抗原を送達する古くからの手法が皮内注射である．インフルエンザHAワクチンにおいて，皮内注射は従来の筋肉内注射と比較して有効性が高いことが報告されている.[4,5] しかし，皮内注射は厚さ数mmの皮膚内に溶液を注入する熟練の技術が必要とされることから，簡便に皮内投与できるデバイスの開発が求められていた．最近，皮内マイクロインジェクションデバイスとして開発されたSoluvia™（Becton Dickinson社）[6]を用いた三価季節性インフルエンザHAワクチン製剤，Intanza®/IDflu®（Sanofi Pasteur社）が上市され，皮膚を標的としたワクチンの有用性が示されつつある.[7] しかし，Intanza®/IDflu®は抗原溶液が充填されたプレフィルドシリンジと使い捨てのマイクロインジェクションデバイスを連結して使用するものであり，従来の注射ワクチン製剤と同様に抗原溶液のcold chainが必要とされるとともに，医療廃棄物処理における費用と危険性が懸念される．また，長さ1.5 mmの針を用いるために投与の際に痛みを伴うという欠点があり，より低侵襲な手法でワクチン抗原を角質層下へと確実に送達できる経皮投与デバイスの開発が望まれている．

3. 経皮ワクチンデリバリー技術の発展

3-1. Electroporation Electroporationは，皮膚への電圧負荷により角質層に一時的に孔をあけて抗原を皮膚内へ送達する物理的経皮送達手法の1つである.[8] 本手法の特徴は，電圧パルスによって細胞膜の構造が緩むことから，様々な皮膚細胞内へ直接抗原を導入できることであり，特にDNAを用いたワクチンにおいて効率的に免疫応答を誘導できる．動物モデルにおいてElectroporationを用いた経皮ワクチンの有効性は多数示されており，[9-11] 注射製剤に比べて低侵襲な手法であることからヒトへの適用が期待されている．しかしながら実用化に向けては，Electroporationの装置が特殊かつ巨大であるためにコストが高いことが大きな課題となっている．

3-2. Jet injector Jet injectorは針を用いずに，空気の圧力によって抗原を皮膚内へ送達する手法である.[12] 針を介した二次感染の危険性がなく，迅速な大規模接種を可能にすることから，軍隊での使用を目的に開発された．日本においても1970年代に小・中学校の予防接種に用いられた実績を有するが，神経線維の損傷が多発したことや痛みが大きいことを受け，既に使用は取りやめられている．現在ではより安価で簡便に扱えるJet injectorの開発が進められ，臨床試験において様々な感染症に対する有効性が報告されており，[13-15] 臨床での定着・普及に向けて安全性の担保が重要課題である．

3-3. 弾性リポソーム 角質層を突破する手法の1つとして，毛包や汗腺を利用した経皮送達が挙げられる．その代表例がナノ粒子であり，近年では特に弾性リポソームの開発が精力的に行われている.[16] 弾性リポソームは脂質や界面活性剤から形成された柔軟な二重膜を有しており，従来のリポソームと比較して皮膚付属器官だけでなく角質層間隙の透過も容易になるとされている．また，ナノ粒子を用いた経皮ワクチンデリバリーは，抗原とアジュバントの両物質を同じ粒子に内包することが可能であり，免疫応答を効率的に活性化できる.[17] 実用化に向けては，脂質や界面活性剤の種類，またその比率を適切に調製することで，ワクチン効果を発揮するに十分な抗原量を送達できる弾性リポソームの開発をしていかなければならない．

3-4. パッチ型製剤 特殊な装置を必要とせず，まさに皮膚に貼るだけという簡便な操作で抗原特異的な免疫応答を誘導できる粘着性パッチ及びガーゼパッチの研究開発がIOMAI社（2008年にIntercell社により買収）及び国立感染症研究所により報告されている.[18,19] これらの経皮ワクチン製剤

は抗原を十分に浸透させるために，角質層あるいは角質層脂質成分を部分的に除去する前処理を必要とする．さらに，ガーゼパッチを応用した経皮ワクチン製剤は，皮膚に適用する直前に抗原溶液を浸み込ませるため簡便性に欠けており，また注射ワクチンと同様に抗原溶液の cold chain を必要とするなど，開発途上国へのワクチン普及を推し進めるためには更なる改良を加える必要がある．

筆者らがコスメディ製薬株式会社と共同開発した親水性ゲルパッチを応用した経皮ワクチン製剤は，皮膚の前処理をすることなく抗原特異的な抗体産生を誘導できる点で画期的である．[20-25] 親水性ゲルパッチはアクリル酸エステル系粘着基剤をベースに，湿潤剤，吸収促進剤など既に医薬品や化粧品などで用いられている安全性の高い材料を配合して作製している．また，本パッチの皮膚貼付面に抗原タンパク質水溶液を滴下すると，水分のみが高分子ゲル体に吸収されてパッチ表面に抗原タンパク質の濃縮層が形成される．このように，抗原を含浸させた状態で取り扱うことができるために輸送・保管が容易になると考えられ，既に破傷風・ジフテリアトキソイドをワクチン抗原として含浸させた経皮ワクチン製剤については，臨床研究においてヒトにおける安全性・有効性を実証している．[24] わが国では多くの人が，乳幼児期の破傷風・ジフテリアトキソイドワクチンの接種により抗トキソイド抗体を有している．その抗体価は年齢を重ねるとともに低下すると言われており，皮膚に貼るだけと簡便な手法でブースト免疫を誘導できる本製剤は非常に有用な新規ワクチン製剤であると言える．

しかしながら，筆者らの親水性ゲルパッチをもってしても角質層下に送達される抗原量は含浸させた量の数％程度であり，[25] 注射と比較すると抗原の利用率が圧倒的に低いことが課題として残されている．そのため，簡便かつ安全なだけでなく安価でより有効なパッチ型経皮ワクチン製剤の実用化に向けては，抗原の角質層透過効率に優れるゲルパッチの改良や免疫増強効果を図るために経皮ワクチン用アジュバントの探索を進める必要がある．

4. マイクロニードル法

マイクロニードル法は，微小な針により角質層に孔をあけることで物質を皮膚内へと送達する手法である．マイクロニードルは長さ 1 mm 以下の微小針であり，神経終末が存在する真皮の深部にまで針が到達しないことから痛みを伴わず，また貼るだけという簡便な操作でワクチンを接種できる．マイクロニードルは，1976 年にその概念が Gerstel と Place らによって報告されて以来，[26] 製造技術が困難であることから費用対効果の面が問題となり，開発研究は停滞していた．しかし，1990 年代になって微細加工技術が発展したことで，現在では様々なマイクロニードルの開発が進められている．

4-1. ソリッドマイクロニードル　ソリッドマイクロニードルはシリコンや金属などで作製された剣山のような微小針であり，これを貼付することで生じた穿刺孔を介してワクチン抗原を皮膚内へ送達することができる［Fig. 2(A)］．[27] ワクチン抗原を塗布する前にマイクロニードルを貼付するだけで，無処置の皮膚と比較して高い抗体産生を誘導できることが確認されている．[28] また，皮膚にワクチン抗原を塗布した後にマイクロニードルを用いて皮膚表面を軽く引っ掻くことで，痛みなく免疫応答を惹起できる手法も報告されている．[29] これらのマイクロニードル前処置あるいは後処置による経皮ワクチンは簡便な手法であるが，ワクチンの皮膚内へのデリバリーはマイクロニードルによる穿刺孔を介した受動拡散に依存するため，ワクチンの投与量やデバイスの貼付時間などの設定が難しいという課題がある．

4-2. 中空マイクロニードル　中空マイクロニードルは，注射針と同様にニードルの中心に空洞がある微小な針であり，シリンジやポンプを用いることで，その空洞を通して皮膚内の特定部位に一定量のワクチンを注入できる［Fig. 2(B)］．ヒトにおいて，インフルエンザ HA ワクチンを中空マイクロニードルにより経皮投与することで，従来型の筋肉内注射による投与よりも少ないワクチン抗原量で同等の有効性を発揮することが報告されている．[30] 本デバイスの実用化に向けては，注入したワクチンが皮膚内から漏れ出さないように，投与部位の深さや投与速度を最適化する必要がある．

4-3. コーティングマイクロニードル　ソリッドマイクロニードルや中空マイクロニードルを用いた手法では，ワクチン抗原を含む溶液を用いるために，現在の注射ワクチン製剤と同様に cold chain を必要とする．開発途上国におけるワクチン普及を推進するためには，この課題を克服しなければなら